JNC TN9400 2000-100

Simulation of Premixing Experiment QUEOS by SIMMER-Ⅲ

June 2000

O-ARAI ENGINEERING CENTER

JAPAN NUCLEAR CYCLE DEVELOPMENT INSTITUTE

Ⓝ

JNC TN9400 2000 – 100
June, 2000

Simulation of Premixing Experiment QUEOS by SIMMER-III

Xuewu CAO*, Yoshiharu TOBITA*

Abstract

The QUEOS, an experiment of the premixing phase of fuel coolant interactions (FCIs), in which several kilograms of solid molybdenum spheres with low temperature (Q-8 300K) and high temperature (Q-12 2300K) are released into water, are simulated to evaluate the drag correlations between the fuel and coolant liquid on the mixing region in FCIs, by SIMMER-III code, in which Ishii's drag correlations in dispersed two-phase flow are employed. The calculated results suggest that the momentum exchange between the spheres and coolant liquid is overestimated in the hot sphere cases by employing the current drag correlations. The difference of the advancement of the sphere cloud between experiments and simulations induced by the drag coefficients is discussed through the change of the multiplier of the drag coefficients.

* Nuclear system Safety Research Group, System Engineering Technology Division, O-arai Engineering Center, JNC

QUEOS実験のシミュレーションを通じたSIMMER-IIIのFCI関連モデルの検証　（その１）

（研究報告書）

曹　学武*、飛田　吉春**

要　旨

QUEOS 実験では１０kg 位の高温（Q-12 ２３００K）又は低温（Q-08 ３００K）の金属粒子を水中に落下し、FCI の粗混合過程が研究されている。この実験のシミュレーションを通じて、SIMMER-III の FCI に関わる粒子抵抗係数モデルの検証を行う計画である。本報告では粒子集団のフロントの位置を実験結果と比較することにより、運動量交換関数の妥当性を検討した。この結果、SIMMER-III は粒子と水の間の運動量交換を高温粒子の場合には過大に評価することが示された。

* 大洗工学センター　システム技術開発部　リスク評価技術開発グループ　博士研究員
**大洗工学センター　システム技術開発部　リスク評価技術開発グループ

Contents

List of figures

1. Introduction

That the high temperature materials (fuel) interact with the low temperature material (coolant) is the important phenomena in nuclear reactor severe accident, which has been numerically studied in recent years. The SIMMER-III code, a two-dimensional, three-velocity-field, multi-phase, multi-component, Eulerian, fluid dynamics computer code coupled with a space and energy dependent neutron kinetics model, developed in JNC [1,2], is being applied to study the fuel coolant interaction (FCI), which needs to extrapolate the constitutive correlations used in the simulation code to describe the FCI processes. The prediction of the premixing region in FCI is important to estimate the consequences of the FCI, which is dominated by the momentum exchange between the fuel and the coolant liquid. In the premixing phase, that the droplets of the fuel moving in the coolant liquid are surrounded by vapor film is featured. Currently employed drag coefficient correlations in SIMMER-III code are those developed by Ishii [3] for two-phase flow. The applicability of those correlations on the premixing phase of FCI, in which droplets are surrounded by vapor film will be estimated through the simulation of the premixing experiment QUEOS [4,5].

The QUEOS experiment has been simulated by other mathematical models, for example, PM-ALPHA [6], IVA-KA [7] as the verification of their models. Due to the advantages of the fixed particle size and long range of temperature from room temperature to 2300 K, the experiment Q-08 and Q-12 are selected to estimate the influence of the drag correlations between the fuel and the coolant on the mixing region. The influence of the fuel temperature on the momentum exchange between the fuel and the coolant liquid will be estimated through the simulation of these two experiments. In this study the pressure transient, the shapes of the particle cloud and the penetration behavior of the particle cloud in water are calculated to estimate the influence of the drag correlations between the fuel and the coolant on the mixing region.

2. Description of experiment

As shown in Fig. 1, the QUEOS facility, as described in [4,5] consists of the test vessel, the furnace and the valve system separating the vessel and the furnace. The solid molybdenum spheres are heated in an electric radiation furnace in an argon atmosphere. After the pneumatically activated release of the spheres, they fall onto a heat-resistant sliding door valve and stay there for less than one second. During this time, the top

valve is closed gas tight and the lower one is opened. Then the middle valve opens symmetrically to two sides within 40 ms and the spheres are discharged into the water with a drop height of 130 cm. The diameter of the sphere stream is 100 mm after the discharge from the middle valve and the spheres fall freely without touching any walls.

The water vessel is made of stainless steel frames and glasses and has a square cross section of 0.7 meter side length and is 1.38 meter high. Three walls have glass windows, with a field of view of 50 by 113.5 cm. A reference grid of 10x10 cm is mounted close to the inside of each of the windows, consisting of steel wire with 2 mm diameter. The fourth wall is instrumentation wall made of steel. At its upper end, there is an opening of 100 mm diameter, connected to the steam venting pipe. The pipe is guard-heated and insulated to prevent condensation. The venting pipe restricts the outflow of the steam from the vessel and therefore the pressure increase in the vessel is both a function of the vaporization rate and flow resistance of the steam pipe. The total pressure loss coefficient, defined as $\zeta = \Delta p/(\rho v^2/2)$, was measured with steady state air flow being $\zeta = 4.54$, with the density ρ of steam and the average velocity v in the pipe. The test vessel is filled with water (0.5 m^3) to a level of 1 m. The water is heated externally. All sides of the vessel are heated from outside by radiators, to obtain a uniform temperature of the water. The bottom of the vessel is covered with 49 (a matrix of 7x7) square boxes (10x10x5 cm) for determining the final distribution of the spheres.

The temperature of water and steam are measured by Ni-CrNi-thermocouples. Six piezoresistive pressure transducers measure the vessel pressure. They are installed at various positions below and above the water level within a shielding tube, which extends 20 mm into the water. In the steam venting pipe, the pressure is measured by miniature piezoresistive transducers 160 cm before the vortex flow meter. The steaming rate is measured by a vortex flowmeter, which works on the principle of vortex shedding. The water level is measured by two impedance level meters positioned in opposite corners of the test vessel.

Experiment Q-08 was performed with the molybdenum spheres with an initial temperature of 300K. 10 kg molybdenum spheres, rested for almost a minute on the middle valve, were released into water pool. The first spheres start to fall at 0 second from the height of 1.3 m above the water surface. The last spheres start to fall at 0.04 second from the height of 1.38 meter above the water surface. The time of free fall of

the first spheres in air 0.015 second. The spheres reach the water surface at 0.515 s and the last spheres reach the water surface at 0.57 s. The corresponding impact velocities are 5.05 m/s and 5.2 m/s for the first spheres and last spheres respectively. When the sphere cloud contacts the water surface, the shape of the cloud was almost a cylinder with a height of 28 cm and a radius of 9 cm. The mean sphere volume fraction was estimated as 0.17 by Meyer [5], although the volume fraction is not uniform, especially at the front and the top of the sphere cloud. There is a large gas volume being dragged deep down into water, when the sphere cloud penetrates into water. The water in the vessel was heated to near the saturated temperature.

Experiment Q-12 was performed with the same molybdenum spheres as Q-08 but with an initial temperature of about 2300K. Because of the high temperature, some of the spheres stuck together within the furnace so that only 6.9 kg were released. The cylinder of the sphere cloud was elongated compared with the theoretical value when it contacts the water surface. The other conditions are the same as the Q-08 experiment.

3. SIMMER-III Representation

3.1 Geometry, initial conditions and calculation system

The QUEOS experimental vessel, shown in Fig.1, is modeled as an axis-symmetric cylindrical volume with the same cross sectional area as the real vessel in a diameter of 0.8 m and the height of 1.4 m. The computational domain employed is shown in Fig. 2, which is a cylindrical vessel and open to outside from the hole with a radius of 0.06 m at the center of the top of the vessel. The simulation starts from the impact of the sphere cloud on the water by a sphere cylinder located at the place 0.056 m above water surface with an initial velocity, slightly less than the value, as described in the report of the experiment by Meyer [4]. The cylinder of spheres with an initial volume fraction of 0.17 has a height of 0.28 m and a radius of 0.09 m, which are estimated by Meyer [5] from the pictures of the images. The front (bottom) of the cylinder of the cloud of the spheres falls to the water level with the initial velocity of 5 m/s. The shape of the cylinder of the spheres has a little difference in two cases in order to match the initial mass of the spheres, which is 10 kg and 6.9 kg in experiments Q-08 and Q-12, respectively. Due to some not yet fully understood mechanisms (possibly some sticking above the sliding doors), the sphere cloud was much longer when contacting the water pool. Although the height of the sphere cloud cylinder in Q-12 is larger than that in Q-08, the same height

of the sphere cloud cylinder is assumed in two cases. The top and bottom radius of the cylinder in Q-12 case is smaller than those in Q-08 case. The volume fraction of the sphere cloud is not uniform along the radial direction. In the center, the value is much higher than that at the boundary. Since the shape and volume fraction distribution could not be clearly determined from the experimental data, in order to avoid too much speculation, uniform sphere volume fraction of 0.17, the same as that in Q08 case, is assumed. In the experiment, 49 square boxes are placed on the bottom of the vessel to determine the distribution of the spheres. This is not simulated in the study, since it does not have much influence on the penetration of the sphere cloud.

In this study, the spheres are molybdenum ball with diameter of 4.2 mm which is the same value with the experiments. The total mass of the molybdenum spheres is 10 kg and 6.9 kg in Q-08 and Q-12 respectively. The initial temperature is 300K and 2300K for Q-08 and Q-12 respectively. The gas space is initially filled with air with initial pressure 1 bar and temperature 370.5 K. The temperature of water in the vessel is assumed as 370.5K.

The geometric model, shown in Fig. 2, is discretized radially by 27 nodes with Δr=0.015 m and axially by 50 nodes with Δz=0.03 (in the water region). The calculations are carried out with a time step of $\Delta t = 4 \times 10^{-5}$ and $\Delta t = 8 \times 10^{-5}$ for Q08 and Q-12 respectively. The initial, minimum and maximum radii of spheres are set to 0.0021 in accordance with the value used in these experiments. 0.001, 0.000001 and 0.0001 are set for the initial, minimum and maximum radii of water respectively. The modified ILUBCG method is selected for fluid dynamics algorithm. The orifices plates are set in the flow-out cells near the center of the top in the calculation domain in order to simulate the venting system in QUEOS experiments. The orifice plate coefficient is 2.27, which is the half of the value measured in the experiments in venting system. The multipliers of the drag coefficient among dispersed components and between dispersed and continuous components are set to 1.0 (default value) respectively. The influence of the drag coefficient by changing the multipliers will be investigated for two cases. The continuous inflow/outflow is set to the boundary cell in the open exit on the top of the domain, in which the pressure is set to constant with 1 bar.

The equation of state for molybdenum is important for the success of the simulation. Here the EOS prepared by Dr. Morita is employed, in which constant density of

molybdenum is assumed.

3.2 Input data set

The input data for the reference calculation is listed in Appendix A.

3.3 Code version and computer used

Calculations are based on SIMMER-III Version 2.F (ALPHA, DBL, URANAS options on). The computer used was an EWS ALPHA.

3.4 Code modifications

No code modifications.

4. Results and discussion

The principle results including pressure transients at the positions corresponding to transducers P2 and P6 in water vessel, water level in the vessel, the evolution of the location of the sphere cloud, the contour graphs of the cloud and mixing region are summarized, in conjunction with the experimental results, in the following. These comparisons focus on the time frame from 0.51 s, at which time spheres contact with the water surface, to 0.8 to 0.9 s, at which the leading edge of the spheres contact the bottom of the water vessel.

4.1 QUEOS Q-08 test base case

In Q-08 experiment, 10 kg molybdenum sphere with 300K was released into water. The pressure transients at the positions corresponding to transducers P2 and P6 in the water vessel, given by the experiments and calculated by SIMMER-III, are plotted in Fig. 3. Generally, the shapes of the calculated pressure transients in P2 and P6 are in agreement with those in the experiment, but the amplitude of the first generated pressure pulse (due to collapse of gas chimney at around 0.75 second) is smaller than those in the experiment. When the cold spheres enter the water at about 0.51 s, the pressure at the position of P6 slightly increases in the water, lasting about 50 ms, then decreases. At 0.72 s it reaches a minimum of 1.05 bar, 20 mbar higher than that in the experiment, then increases and decreases sharply, forms a highest pressure spike of 1.115 bar, 80 mbar less than the value in the experiment. The maximum pressure peak values occurs at the time a little later than that in the experiment, which coincides with the collapse of

the gas chimney formed during the falling of the sphere cloud in the water. In the experiment the high pressure peak reverberates several times with a frequency of 18 Hz and declining amplitude, but in the calculation the reverberation is in a much lower frequency (duration is about 150 ms) and the amplitude slightly higher than that in the experiment. The difference may be caused by not simulating the sphere collection cells on the bottom of the vessel or by the system difference between the real vessel and calculated vessel, which have different inherent frequency. In the experiment, the water vessel is quadratic in cross section and it becomes circle in the calculation. Although the shape of the pressure transient is generally in agreement with that in experiment and the differences are given, it is not enough to be used to estimate the momentum transfer between the spheres and the water during the penetration, which will be further discussed later.

The 0.5 contour line of water volume fraction is defined as the interface of bulk water and the water level swell is plotted as shown in Fig. 4. In the experiment, the water level was measured on the corner of the vessel. Here the calculated water level is the water depth at the position of the place near the radial boundary of the cylindrical vessel. The water level transient shows that the maximum calculated water level occurred at around 0.8 second (instead of 0.7 second in the experiment) are larger than that in the experiment. And then it decreases. The difference may be induced by the definition of the interface and the counted position of the water level. Due to the diffusion of the boundary and the change of the counted position of the water level, the output value changes too much. It is more difficult to compare the calculated value with experimental data.

The contour line of the volume fraction of the sphere cloud with the half (0.085 initially) of maximum value (0.17 initially) of the volume fraction is defined as the interface of the sphere cloud. The leading edge of the sphere cloud is counted, as shown in Fig. 5. The 0.5 contour line of the volume fraction of water is defined as the boundary of the water region and the leading edge of the water is plotted as shown in Fig. 5. Since the leading edge of the sphere cloud is below the leading edge of the water, here the leading edge of the sphere cloud is taken as the leading edge of the mixing region. The spheres penetrated into water and the leading edge of the mixing region moves down at a velocity of about 2.0 m/s in the experiment, as shown in Fig. 5, in which the penetration rate of the cloud is almost linear. The calculated penetration rate is also

almost linear and it is about 2.5 m/s, which is a little larger than that in the experiment.

The evolution of the leading edge of the sphere cloud suggests that the momentum exchange between the solid spheres and the water is overestimated just after the cylinder of the sphere cloud completely enters the water (at about 0.61 s) in the current calculation model. The impact of the sphere on water with a velocity of 5 m/s implies high accelerations of the relative motion of the two phases. For the spheres impact on the water the acceleration term for momentum exchange is negative. Since the virtual term for solid spheres is not considered in the current model, the momentum exchange is overestimated.

The momentum exchange is underestimated after the sphere cloud completely enters the water in current calculation model. In this calculation, the multiplier of drag coefficient is 1.0. The influence of the drag coefficients on mixing region will be investigated later through the change of the multipliers of the drag coefficients. The contour graph of the volume fraction of the sphere cloud and the water in the time of 0.53, 0.59, 0.65, 0.71, 0.77 and 0.83 are plotted in Figs. 6 and 7. The sphere cloud cylinder becomes thinner and wider with evolution. The volume fraction of the sphere cloud becomes larger (larger than the initial value) in the center and smaller in boundary. The figure 7 shows the formation and collapse of the gas chimney. A large bubble is formed in the water. The image of mixing region taken from the experiment is shown in Fig.8, plotted at the same time as the calculated results. The diameter of the mixing region in the calculation is about 0.2 m (0.032 contour line) and 0.24 (0.016 contour line) at the time of 0.77 s. This value is about 0.25 m in the experiment.

4.2 Investigation of the influence of the drag coefficient on mixing region in Q-08 test

The influence of the drag coefficients on the mixing region in the cold sphere experiment is investigated through the change of the multipliers CDD and CCD of the drag coefficient among dispersed components and between dispersed and continuous components. The cases with the multipliers of 0.125, 0.25, 1.0 and 2.0 are investigated and the evolutions of the location of the leading edge of the sphere cloud and water are plotted as shown in Figs. 9 and 10. Due to the underestimation of the momentum exchange, the larger the multiplier, the more the evolution approaches to the experimental data. The evolution of the location of the leading edge of the sphere cloud in the case with the drag coefficient multiplier of 2.0 most approaches to the

experimental data. The calculated results show the multiplier of 2.0 for cold sphere release experiment is suggested. The contour graphs of the sphere cloud and water for the cases with different multipliers are plotted at the time of 0.77 second to see the effect of the drag coefficient on the shape of the mixing region, as shown in Figs. 11 and 12 respectively. For the cases with larger value of the multiplier, the mixing region becomes wider and shorter, and the gas chimney collapses later.

The pressure transients in the vessel at the position of P6 are shown in Fig. 13 for the cases with different multiplier of the drag coefficients. The amplitude of the pressure peak due to the collapse of the gas chimney is not much affected by the drag coefficient, but it affects the occurrence time as shown in Fig. 13. The more cases with different CDD and CCD are calculated, as shown in Fig. 14. The results show that in Q-08 simulation the drag coefficient between dispersed and continuous components (between solid sphere and water) plays an important role.

4.3 Investigation of the influence of gas composition on pressure in Q-08 test

The exact composition of gas in the upper free space of the vessel is not clear in the experiment. Three cases with different gas and vapor composition filled in the free space are investigated. The partial pressures set for air and vapor are 99 KPa and 1 KPa, 99.99 KPa and 0.01 KPa respectively for case1 and 3. For case 2 the gas is Xe and its partial pressure is 90 KPa. The remaining vapor partial pressure is 10 KPa. The pressures at point P6 in each case are shown in Fig. 15, which suggest that the composition of non-condensable gas and vapor in the free space makes the pressure a little change, but no much difference. The initial pressure transient is improved by specifying lower vapor partial pressure.

4.4 QUEOS Q-12 test base case

In Q-12 experiment, 6.9 kg molybdenum sphere with the temperature of 2300K was released into water. The pressure transients in positions corresponding to transducers P2 and P6 in the water vessel, given by the experiments and calculated by SIMMER-III, are plotted in Fig. 16, which suggests that the heat transfer in the water/evaporation process is overestimated in the calculation. When the hot spheres enter the water at time 0.51, the pressure at the position corresponding to P6 increases quickly. It reaches a plateau, which continues about 0.15 s, then it decreases sharply (but not as much as that in the

experiment) and reaches to a level slightly higher than the experiment. A small peak is seen in the calculation, which appears in the experiment due to the collapse of the gas chimney at 0.72 s. In this case the pressure transient shape is similar to the experiment, but the amplitude is slightly larger than that in the experiment and the pressure plateau extends 100 ms longer than that in the experiment, which is induced by higher heat transfer to water and evaporation of water.

In order to estimate the effect of the venting pipe, three cases with different orifice plate pressure drop coefficients are calculated and the results are plotted in Fig. 17. The coefficients of the pressure drop in the orifice are 1.135, 2.27 and 4.54 in three cases respectively. The pressure in the water (P6) is not sensitive to it. It is not the main factor influencing the pressure transient.

With the same definition of the boundaries between the sphere cloud and the water, the evolution of the location of the leading edge of the hot sphere cloud and water and water level swell are plotted as shown in Figs. 18 and 19 respectively. The leading edge of the sphere cloud suggests that the momentum exchange between the hot spheres and the water are overestimated. In the hot sphere experiment, spheres are surrounded by vapor film. The drag force with this configuration is not considered in the current SIMMER-III model. Comparing with the cold sphere experiment, the overestimation of the drag force suggests that the model for the drag coefficient considering the influence of the vapor film should be employed. The experimental data shows that the penetration rate is larger in the hot sphere case than that in cold sphere case, but the current calculation results show the reversed tendency. This also shows the current drag model overestimate the drag force of the spheres with vapor film in the hot sphere experiment. The contour graphs of sphere cloud and water are shown in Figs. 20 and 21, plotted at time 0.53, 0.586, 0.642, 0.754 and 0.81s. The mixing region evolution is larger in diameter than that in the experiment, shown in Fig. 22, plotted as the same time as the calculated results, which induce the same conclusion.

The gas flow rates through the venting pipe given by the experiment and by SIMMER-III are plotted in Fig. 23, which show that the evolution of gas flow rate calculated by SIMMER-III is qualitatively consistent with that in the experiment, but the maximum value is about two times of that in the experiment and the total vapor generation in calculation is larger than that in the experiment. Although the vapor

generation rate, which corresponds to the pressure transient given by SIMMER-III, is affected by several factors, for example, orifice plate pressure drop coefficient, difference of initial gas composition and initial gas space volume, the larger amount of vapor generation suggests that the heat transfer from spheres to water and its evaporation are overestimated during the falling of the hot sphere cloud in the water by SIMMER-III. Since the sphere radius is fixed, the factors influencing the heat/mass transfer process include the heat transfer coefficients from sphere to water/vapor in different flow regime, water/vapor interfacial area and evaporation of water. Through this simulation, the factors could not be distinguished and the more specific experiments are needed to make further investigation.

4.5 Investigation of the influence of the drag coefficient on mixing region in Q-12 test

The influence of the drag coefficient on the mixing region in the hot sphere experiment is investigated through the change of the multipliers CDD and CCD of the drag coefficient among dispersed components and between dispersed and continuous components. The cases with the multipliers (CDD and CCD) of 0.05, 0.25 and 1.0 for Q-12 are calculated. The evolution of the leading edge of the sphere cloud and water are shown in Figs. 24 and 25 respectively. Since the momentum exchange is overestimated by using the default value. The lower the multiplier, the more the evolution of the leading edge approaches to the experimental data. The multiplier of 0.05 is suggested by the calculated results. The contour graphs of the sphere cloud and water are plotted at the time of 0.698 second, as shown in Figs. 26 and 27 respectively. The shapes of the sphere cloud and water region are much affected by the drag coefficient. In the cases with the reduction of drag coefficient of 20 times, the shapes of the sphere cloud approach to the image taken from the experiment.

The pressure transients in the vessel at the position of P6 are shown in Fig. 28 for the cases with different the drag coefficients through the change of the multipliers. The pressure is higher for the cases with lower multiplier of the drag coefficient, which corresponds to the vapor generation rate as shown in Fig. 29. Other cases with different combination of the CDD and CCD are calculated, as shown in Fig. 30. These results suggest that both the momentum exchange between sphere and coolant liquid and the momentum exchange between the sphere and liquid particle are overestimated.

5. Conclusions

The momentum exchange between the fuel and coolant liquid in FCI is estimated through the simulation of the QUEOS experiments Q-08 and Q-12 (the experiment of a premixing phase of FCIs). The base cases are carried out by using the standard options of the models and the parameters in SIMMER-III code. Then the difference of the advancement of the sphere cloud between experiments and simulations induced by the drag coefficients is discussed through the change of the multipliers of drag coefficients. The calculated results suggest:

In the case of the cold sphere experiment QUEOS Q-08, SIMMER-III can predict the behavior of the advancement of the sphere cloud, pressure and vapor generation transient.

In the case of the hot sphere experiment QUEOS Q-12, the momentum exchange between the spheres and coolant liquid is overestimated by employing the current Ishii's drag correlations. The Influence of the vapor film surrounded on the sphere moving in the coolant liquid on the drag correlations should be considered.

6. Recommendations for model improvements

Based on the calculated results, the model improvement is recommended for SIMMER-III. It is better to develop a drag coefficient model based on the configuration that the hot spheres with vapor film move in coolant liquid.

7. References

(1) Sa. Kondo, et al.: Proc. of Eighth International Topical Meeting on Nuclear Reactor Thermal-Hydraulics, Vol. 3, P. 1340, Kyoto, Japan, Sept. 30-Oct. 4 1997.

(2) K. Morita, et al.: Proc. of the OECD/CSNI Specialists Meeting on Fuel- Coolant Interactions. P. 785, May 19-21, 1997, JAERI, Tokai-mura, Japan.

(3) M.Ishii and N.Zuber, Drag Coefficient and Relative Velocity in Bubbly, Droplet or Particulate Flows, AIChE Journal Vol. 25, No. 5 September 1979.

(4) L.Meyer,QUEOS, an Experimental Investigation of the Premixing Phase with Hot Spheres, Proceedings of Eighth International Topical Meeting on Nuclear Reactor

Thermal-Hydraulics, Vol. 3, Kyoto, Japan, Sept. 30-Oct. 4 1997

(5) L.Meyer,G.Schumacher, QUEOS, a Simulation-Experiment of the Premixing Phase of a Steam Explosion with Hot Spheres in Water Base Case Experiments, FZKA Report 5612, Forschungszentrum Karlsruhe, April 1996.

(6) T.Theofanous, W.Yuen and S.Angelini, The Verification Basis of The PM-ALPHA Code, Proceedings of the OECD/CSNI Specialists Meeting on Fuel-Coolant Interactions May 19-21, 1997, Tokai-mura, Japan.

(7) H.Jacobs,L.Vath,K.Thurnay, Constitutive Relations for Multiphase Flow Modeling, Proceedings of the OECD/CSNI Specialists Meeting on Fuel- Coolant Interactions May 19-21, 1997, Tokai-mura, Japan.

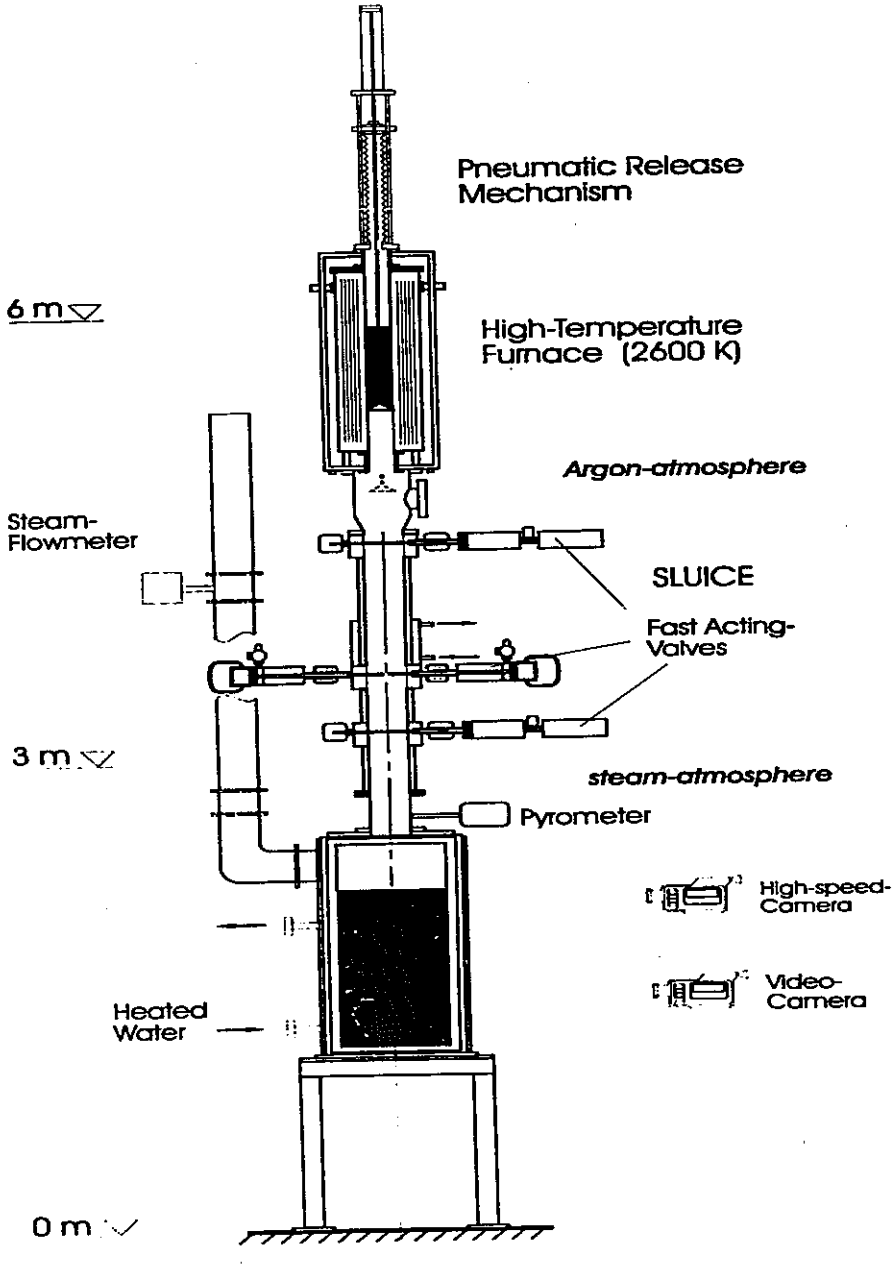

Fig. 1. Scheme of the QUEOS facility

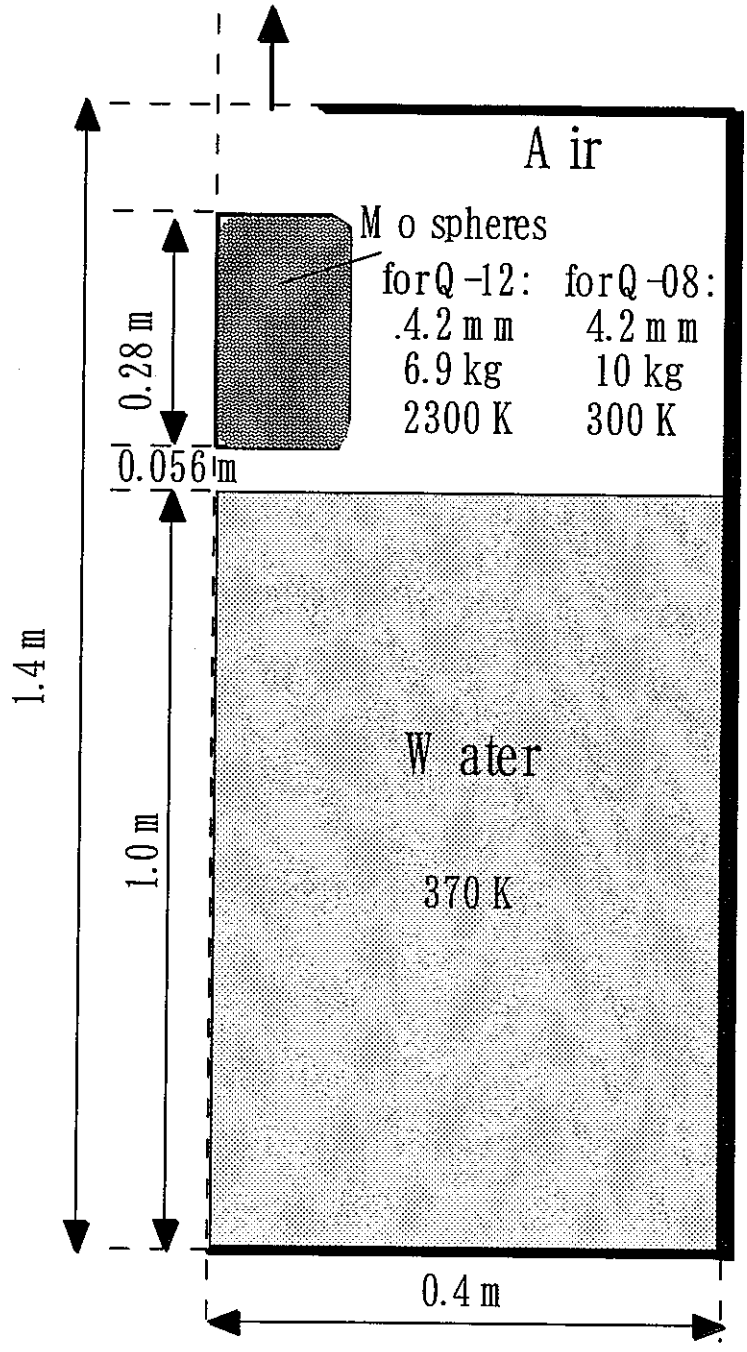

Fig. 2. Simulation Model of QUEOS test

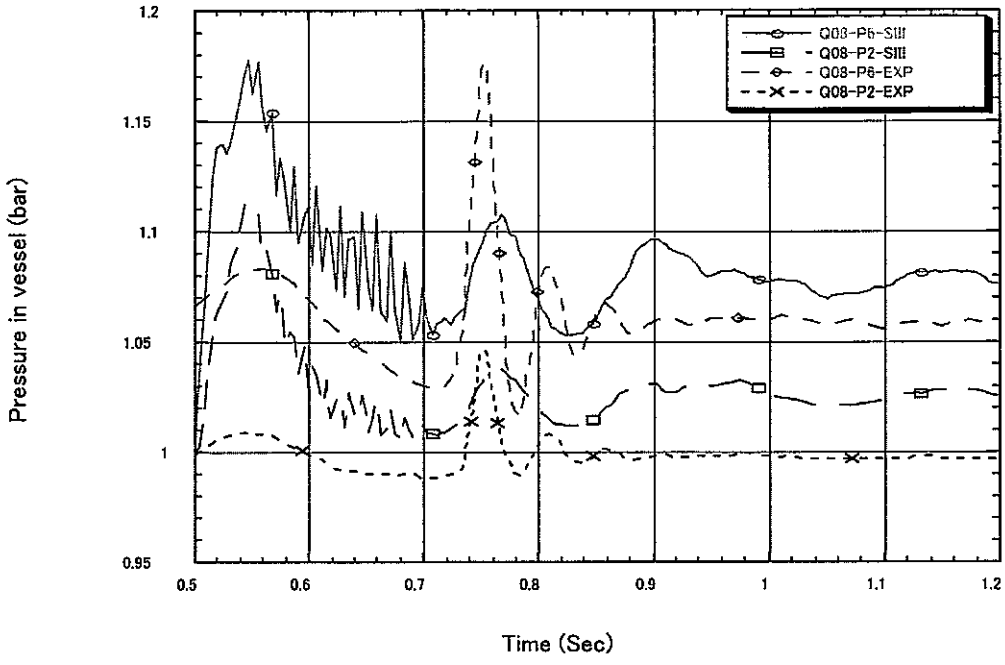

Fig. 3. Pressure in the vessel at position of P2 and P6 in Q-08

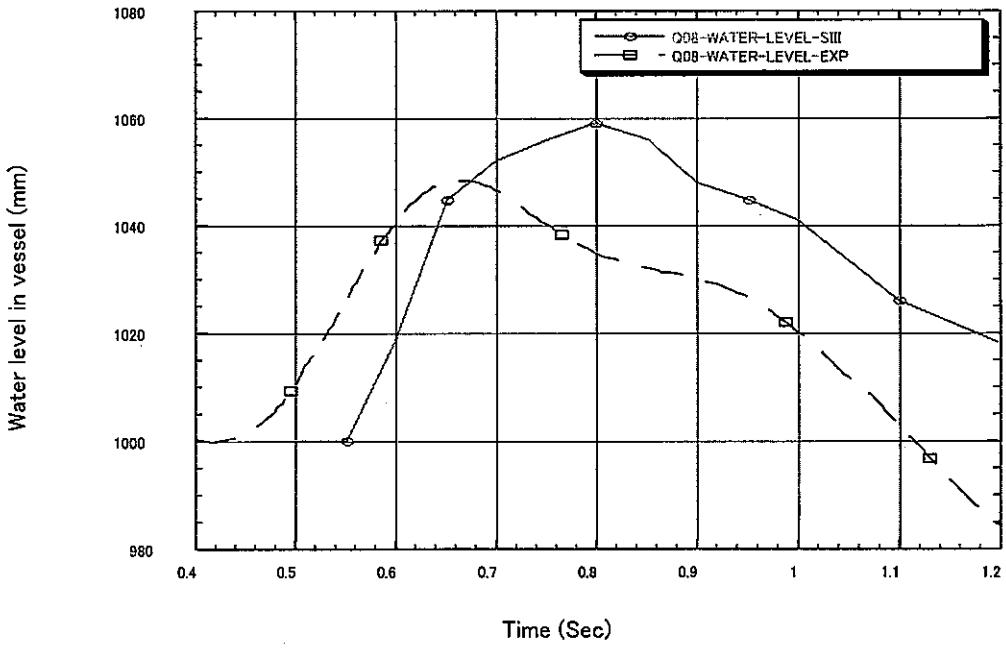

Fig. 4. Water level transient in the vessel in Q-08

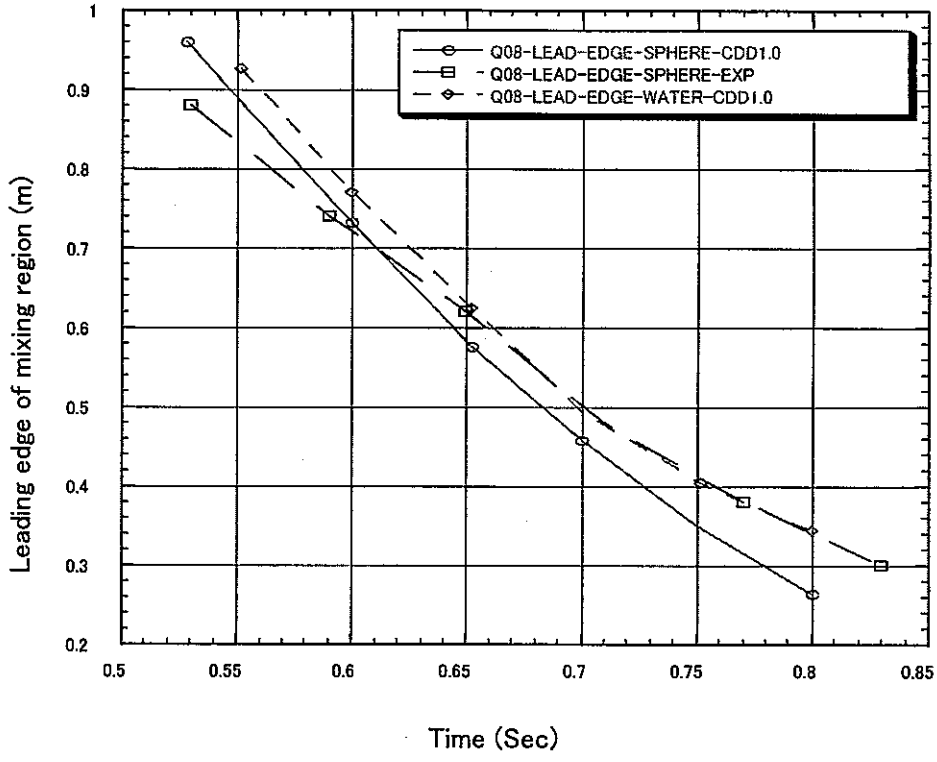

Fig. 5. Evolution of the leading edges of the sphere cloud and water in Q-08.

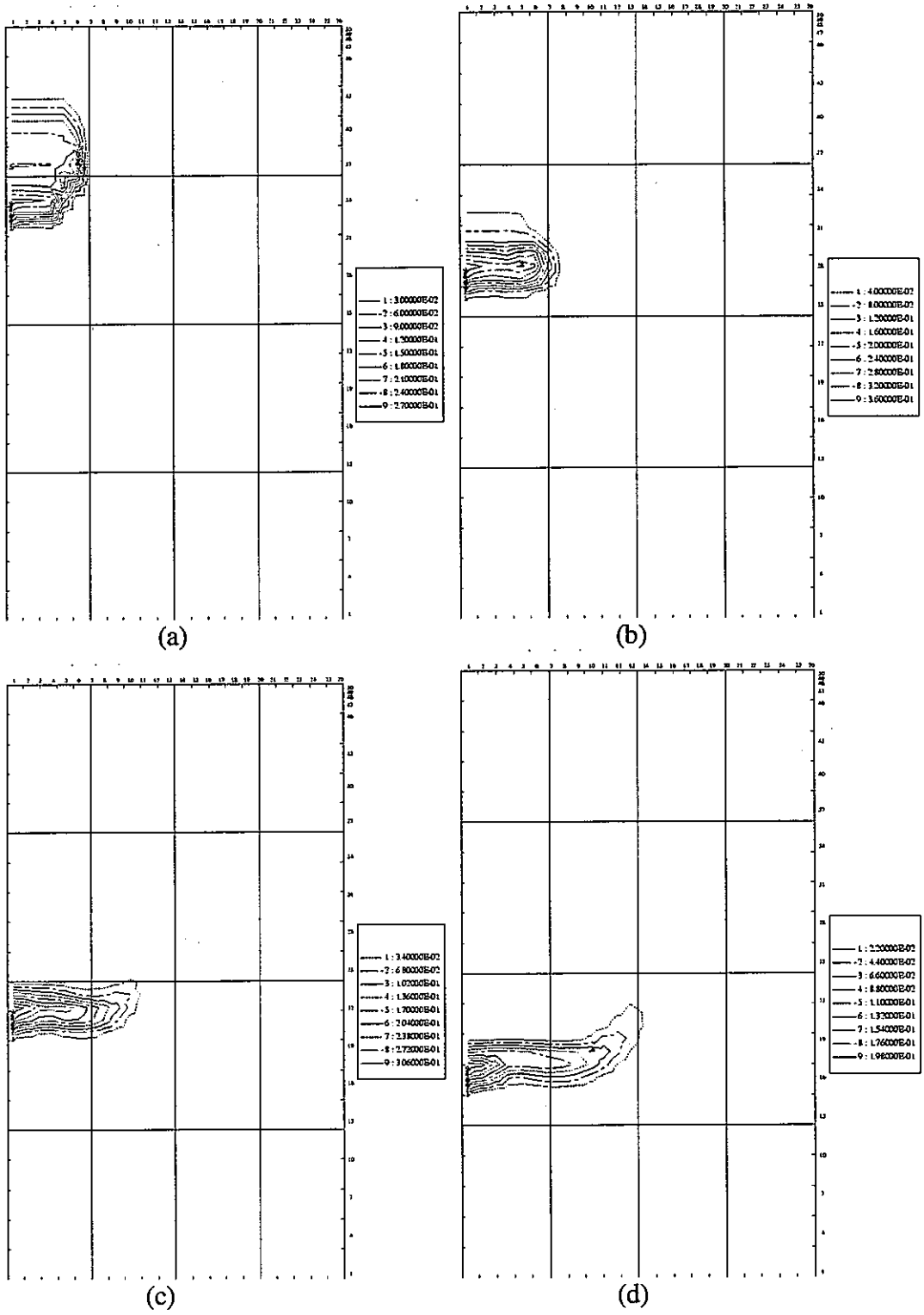
(a)
(b)
(c)
(d)

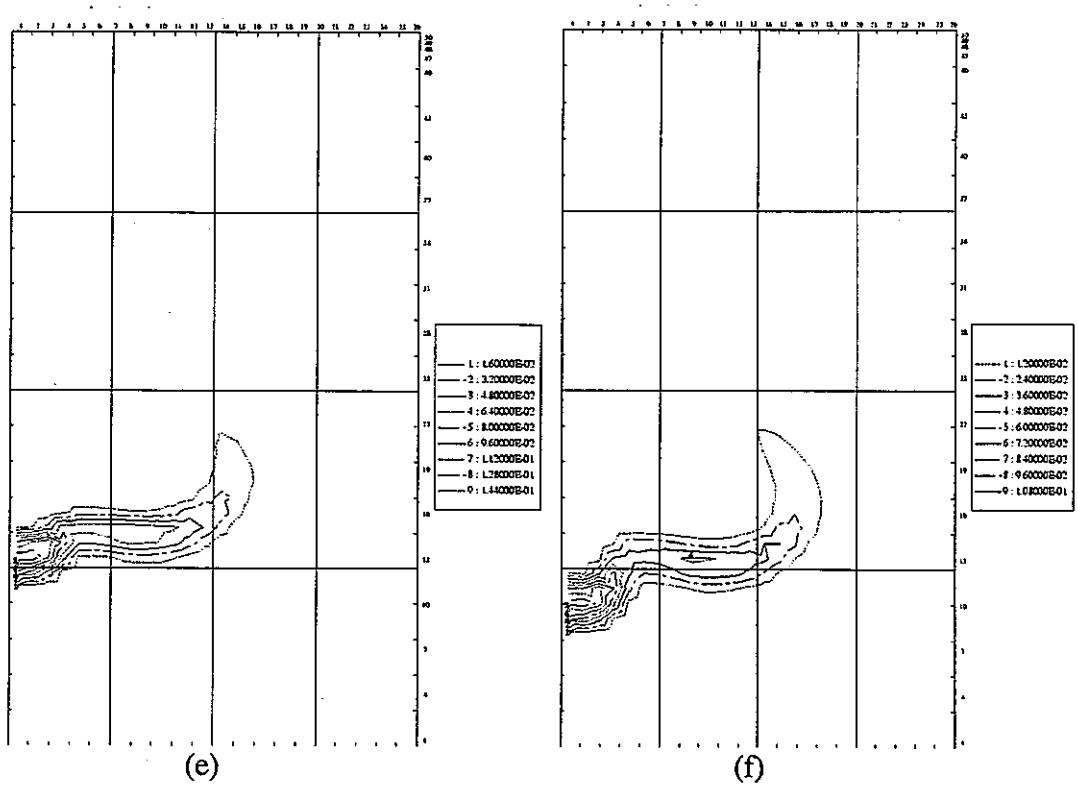

Fig. 6. Contour graphs of the volume fraction of the sphere cloud in Q-08, plotted at time of 0.53, 0.59, 0.65, 0.71, 0.77 and 0.83 second from (a) through (f).

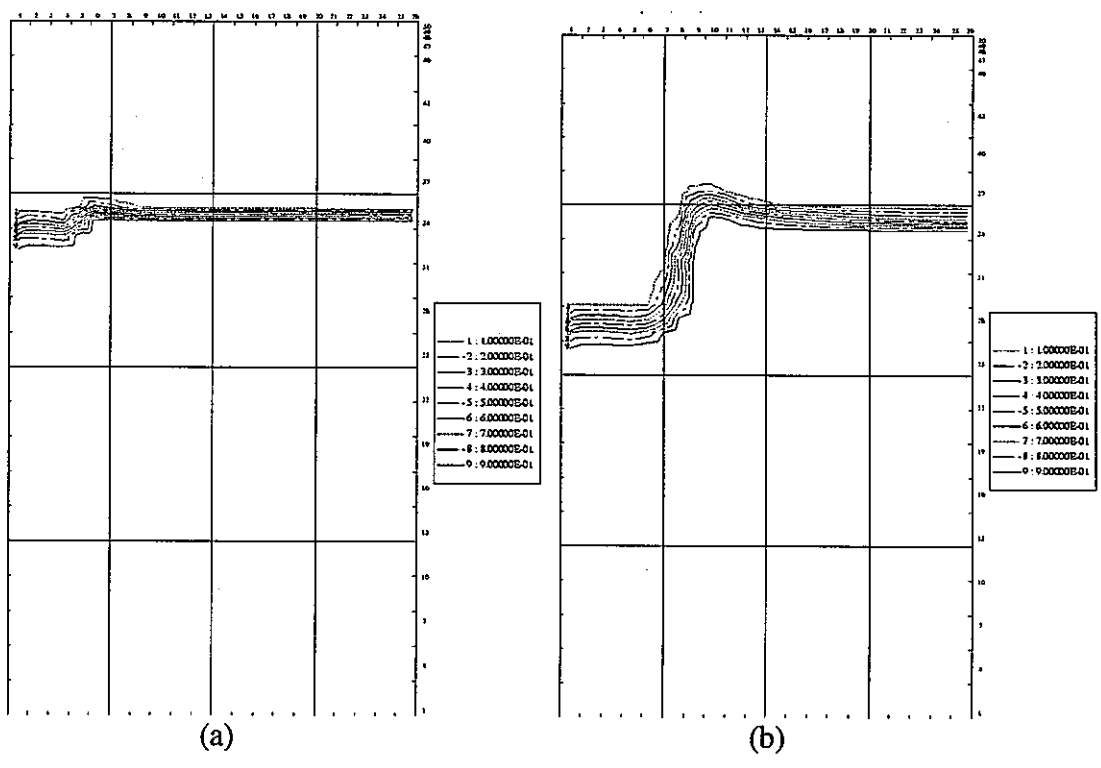

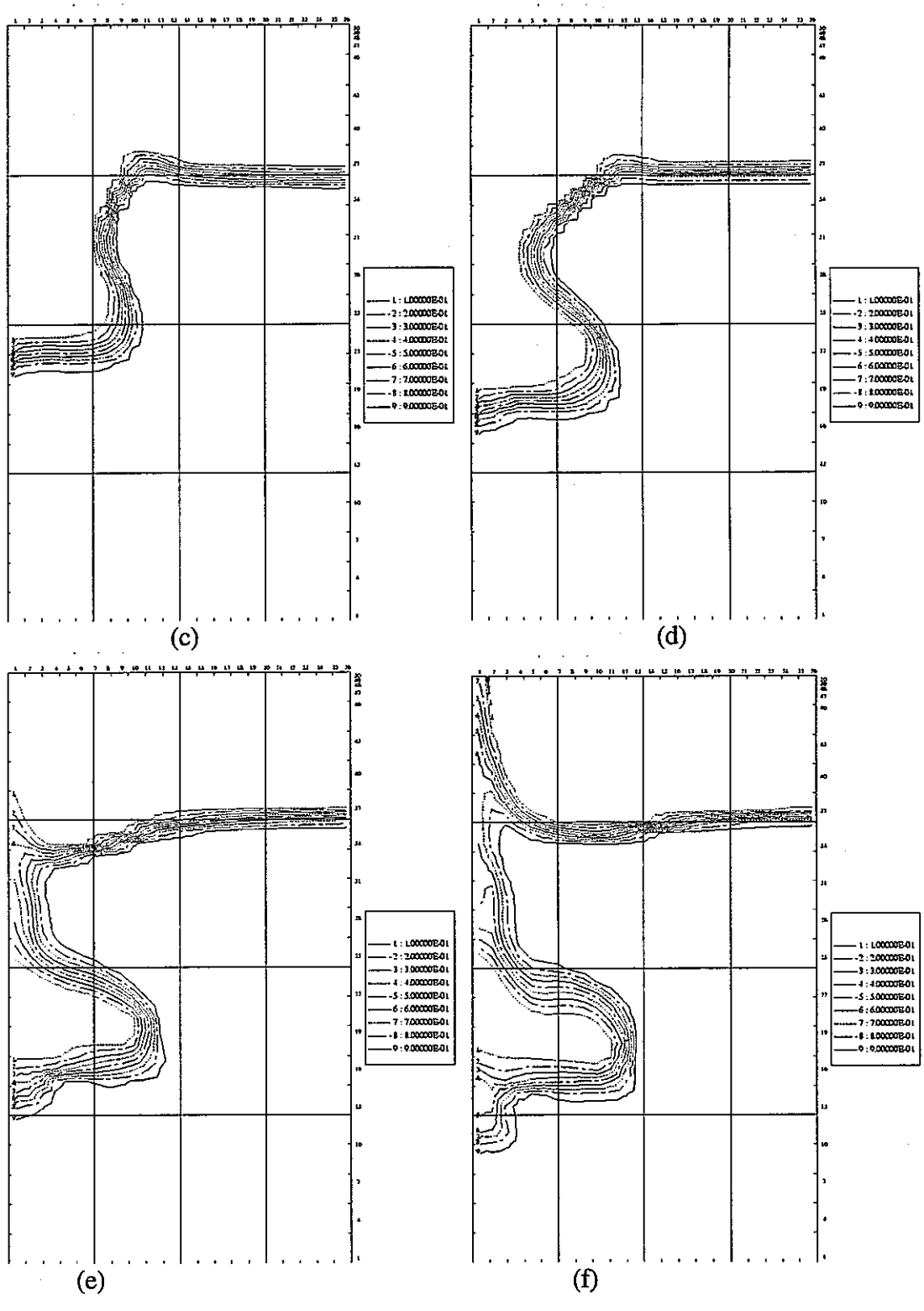

Fig. 7. Contour graphs of the volume fraction of water in Q-08, plotted at time of 0.53, 0.59, 0.65, 0.71, 0.77 and 0.83 second from (a) through (f).

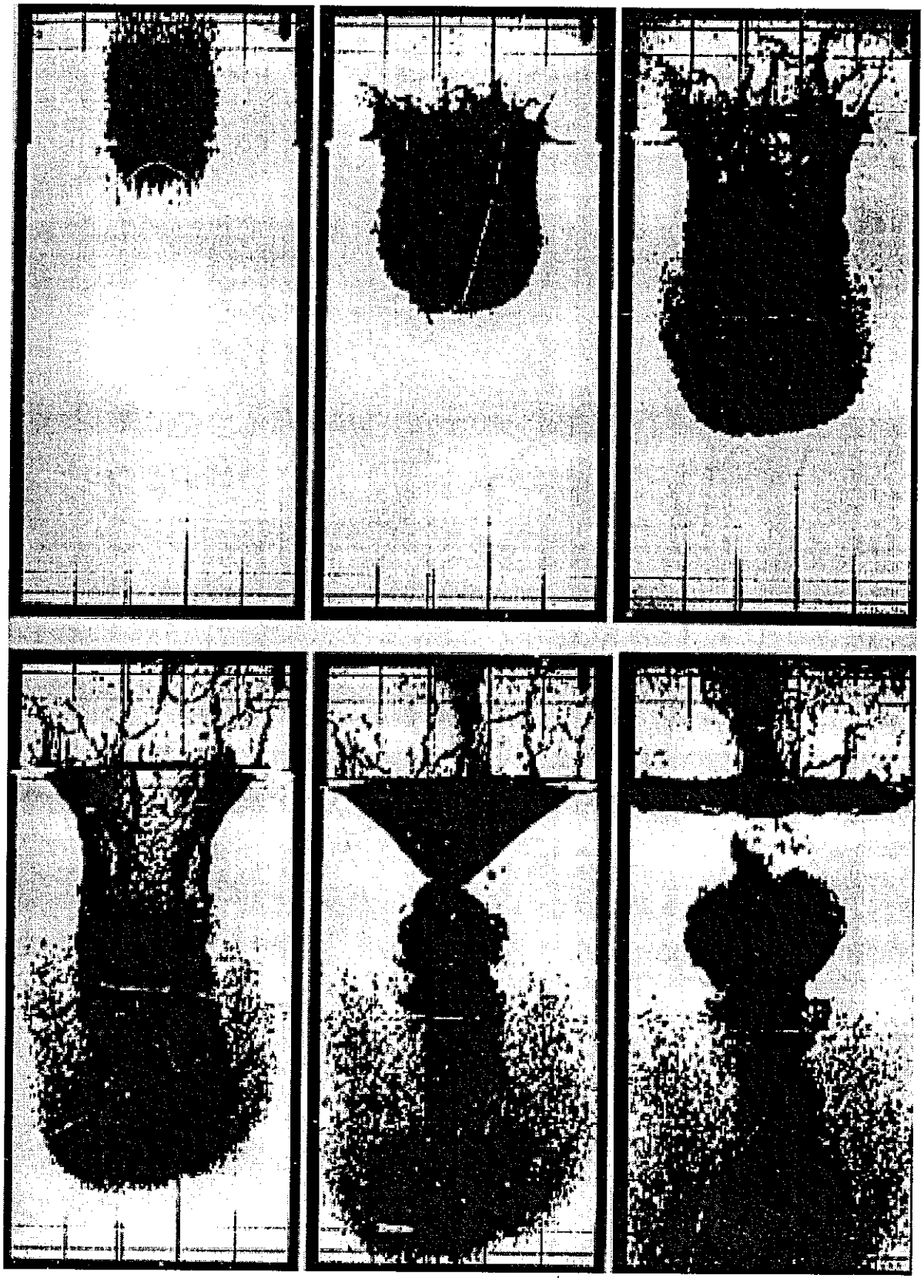

Fig. 8. Images of molybdenum sphere cloud falling in water in Q-08 experiment

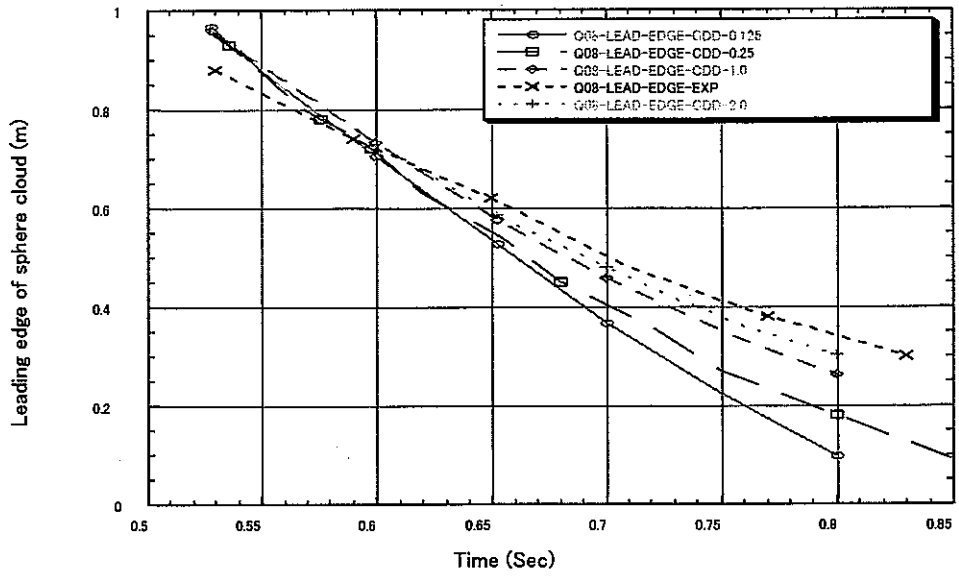

Fig. 9. Evolution of the leading edge of the sphere cloud in cases with different drag coefficient multipliers CDD and CCD of 0.125, 0.25, 1.0 and 2.0 in Q-08.

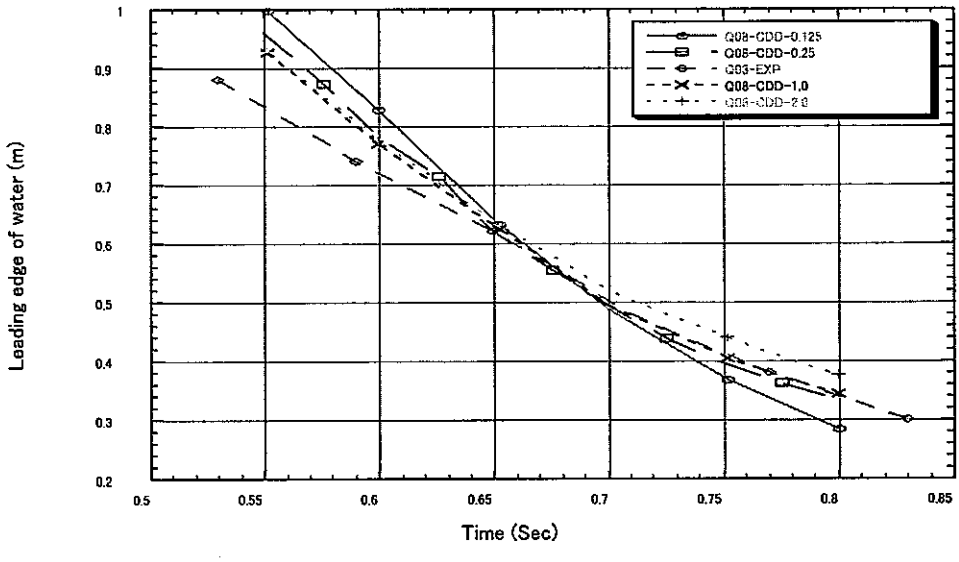

Fig. 10. Evolution of the leading edge of water in cases with different drag coefficient multipliers CDD and CCD of 0.125, 0.25, 1.0 and 2.0 in Q-08.

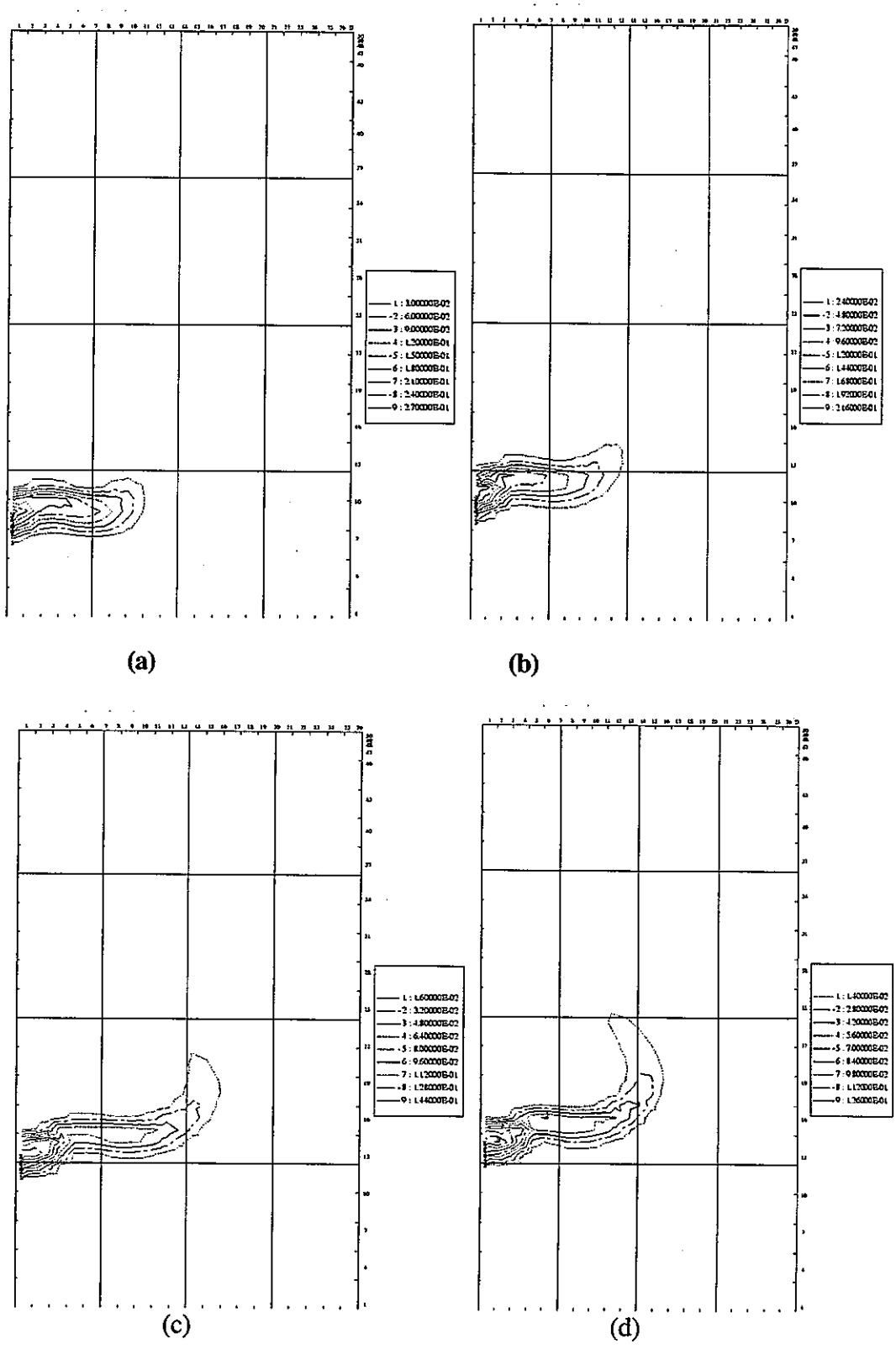

Fig. 11. Contour graphs of the volume fraction of the sphere cloud in Q-08, plotted at time of 0.77 second for the cases with drag coefficient multiplier of 0.125, 0.25, 1.0 and 2.0 from (a) through (d).

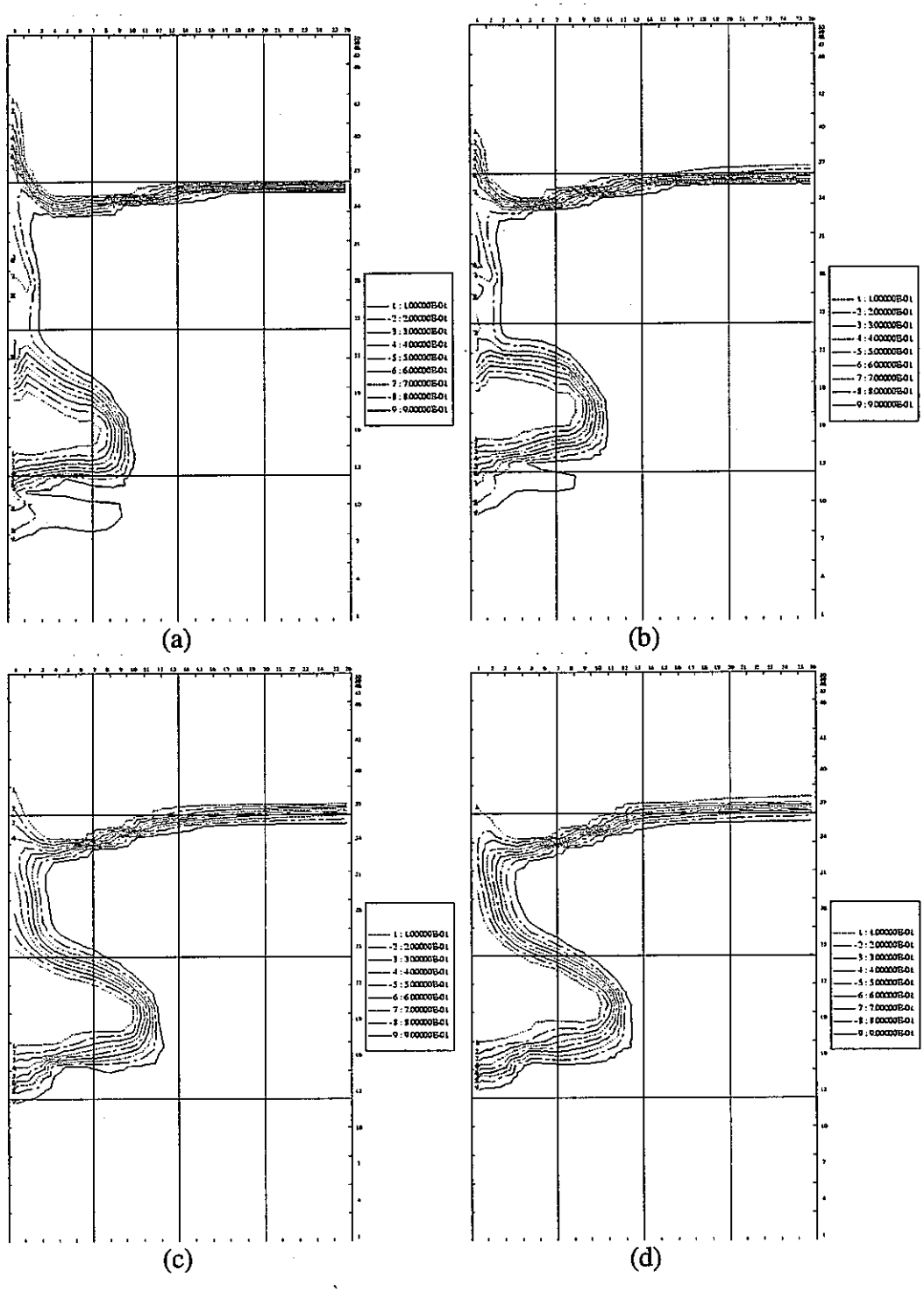

Fig. 12. Contour graphs of the volume fraction of water in Q-08, plotted at time of 0.77 second for the cases with drag coefficient multiplier of 0.125, 0.25, 1.0 and 2.0 from (a) through (d).

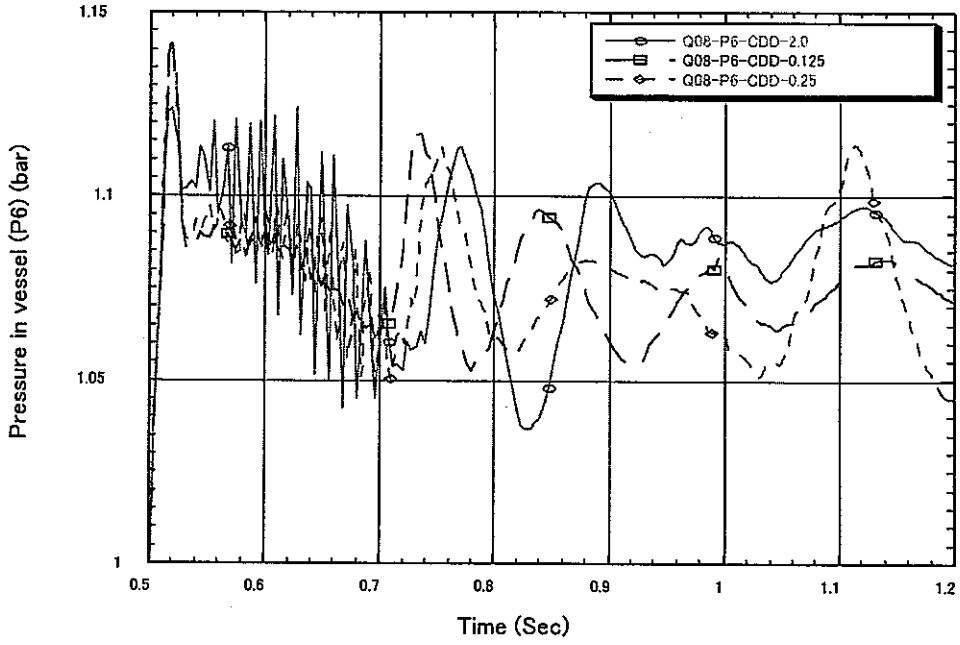

Fig. 13. Pressure transients in the vessel at position of P6 in the cases of Q-08 with different multiplier of drag coefficient

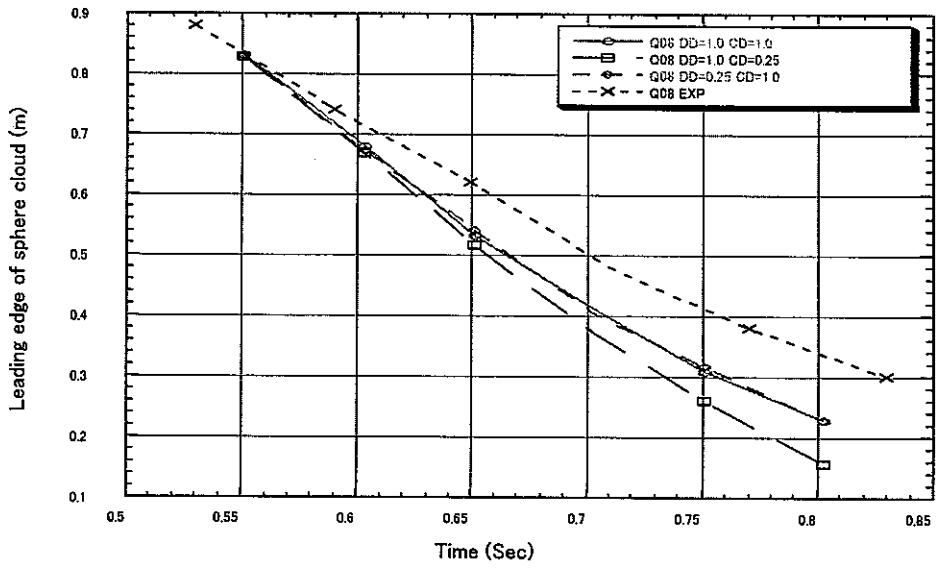

Fig. 14. Evolution of the leading edge of the sphere cloud in cases with different drag coefficient multipliers CDD and CCD in Q-08.

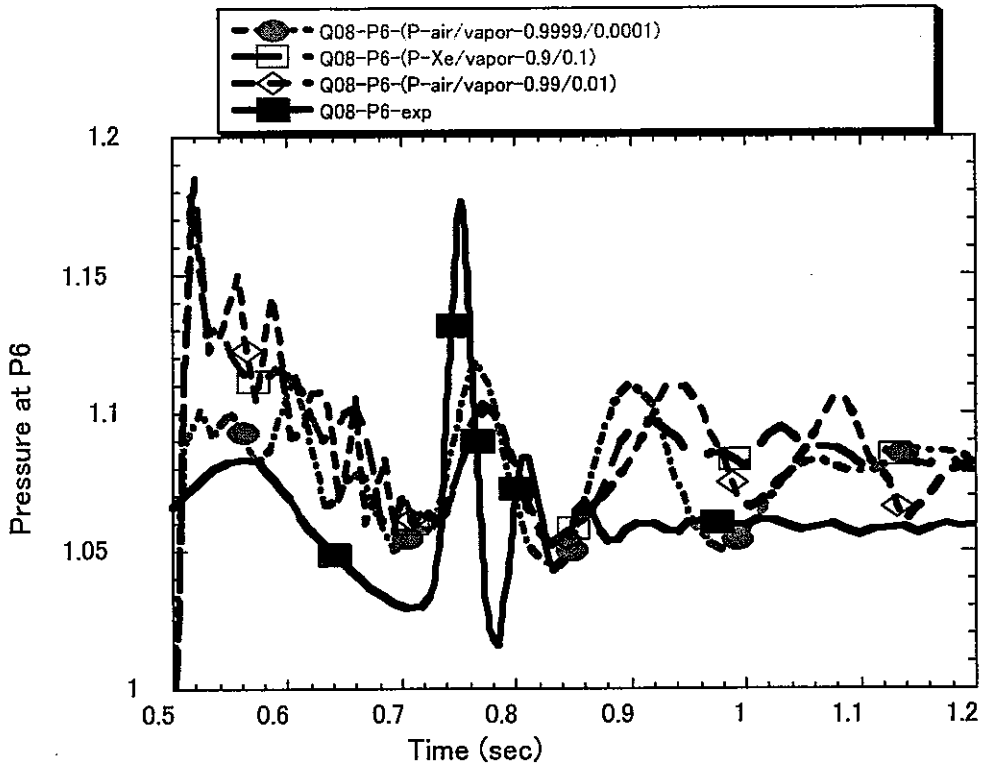

Fig. 15. Pressure transients in vessel at position of P6 in the cases of Q-08 with different ratio of air to vapor in air space.

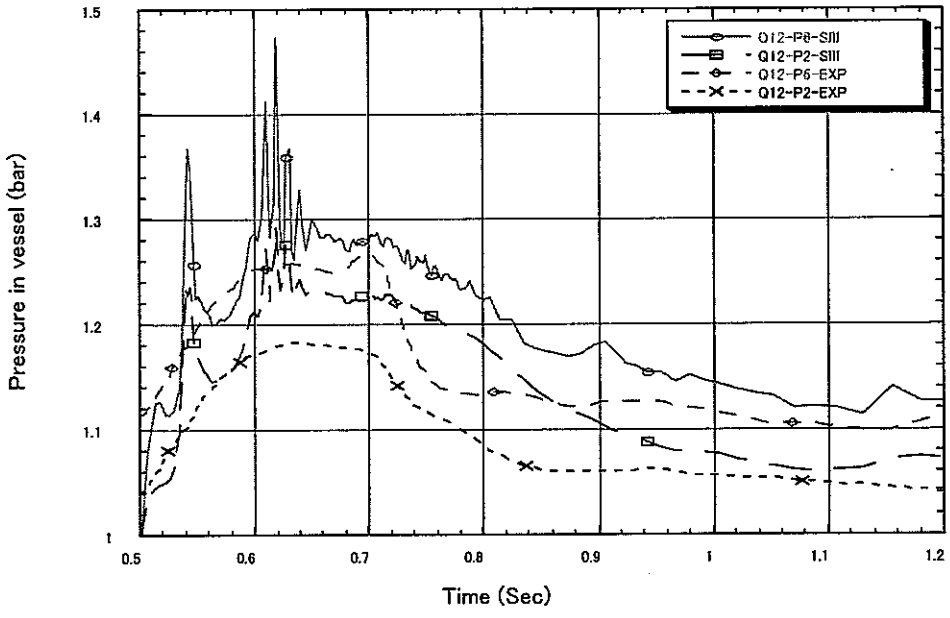

Fig. 16. Pressure in the vessel at position of P2 and P6 in Q-12

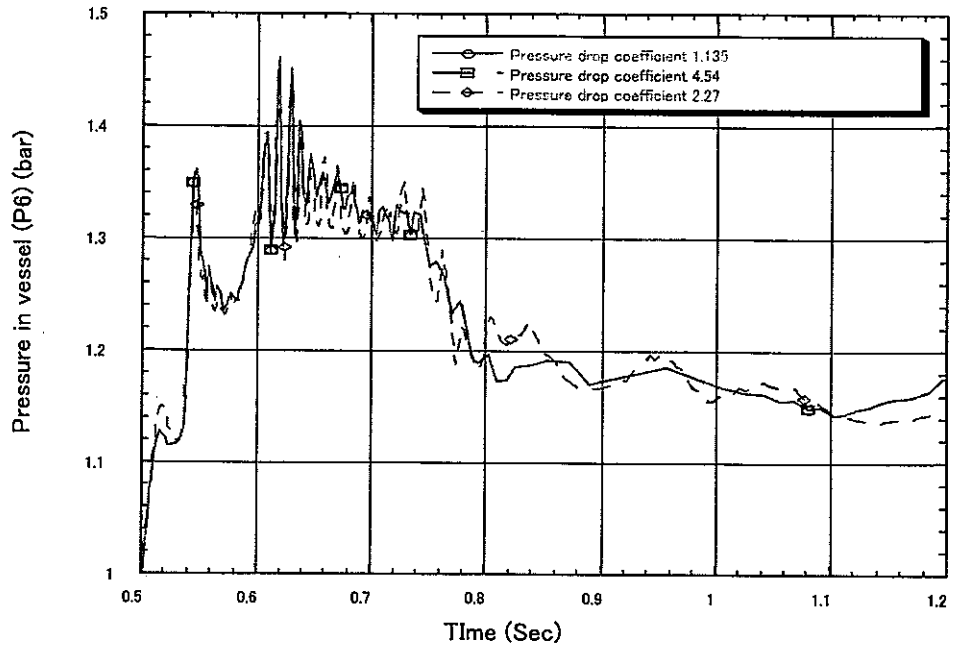

Fig. 17. Influence of pressure drop coefficient on pressure in flow exit in Q-12.

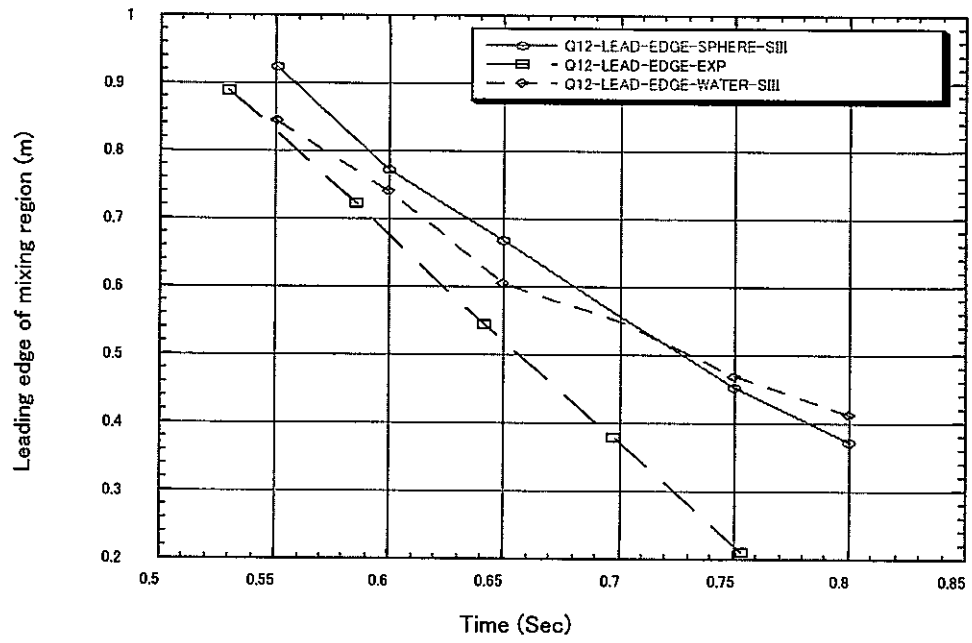

Fig. 18. Evolution of the leading edge of the sphere cloud and water in Q-12, the half of the volume fraction contour line is defined as the boundary of the cloud.

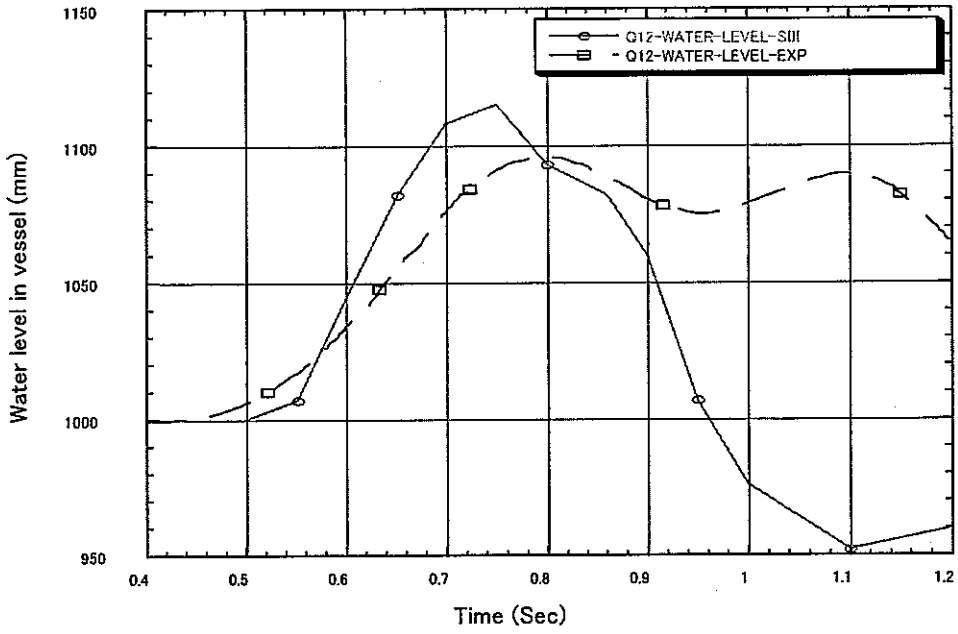

Fig. 19. Water level transient in thevessel in Q-12

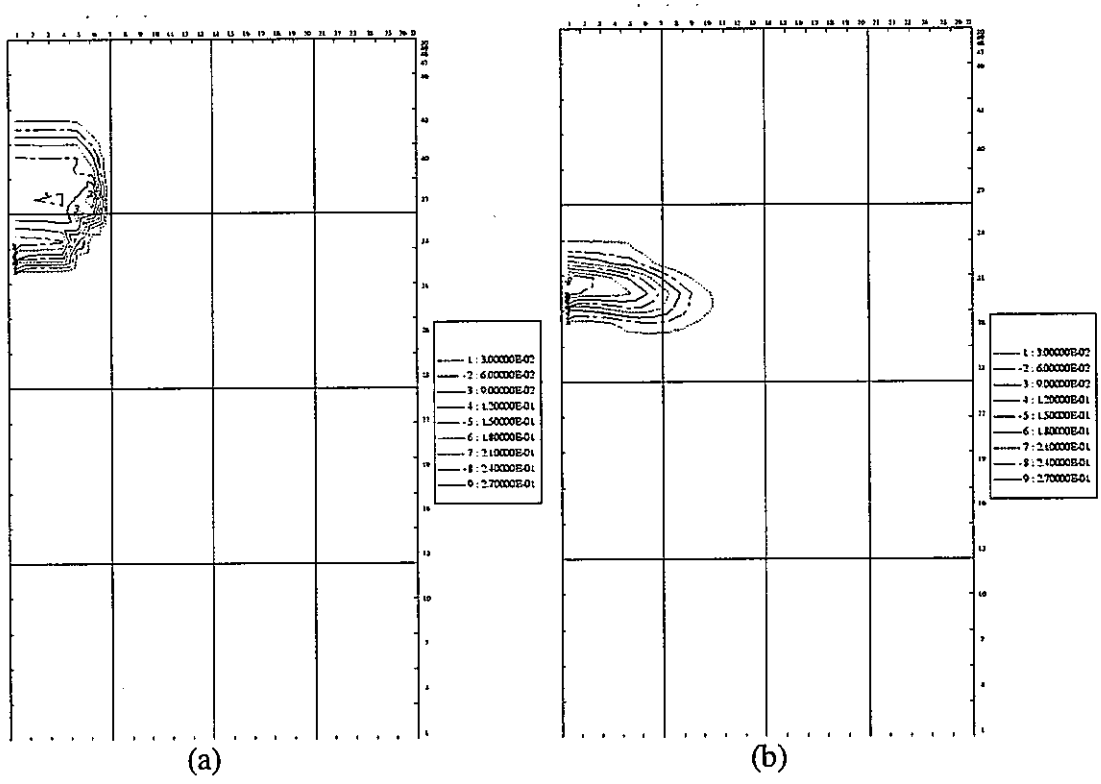

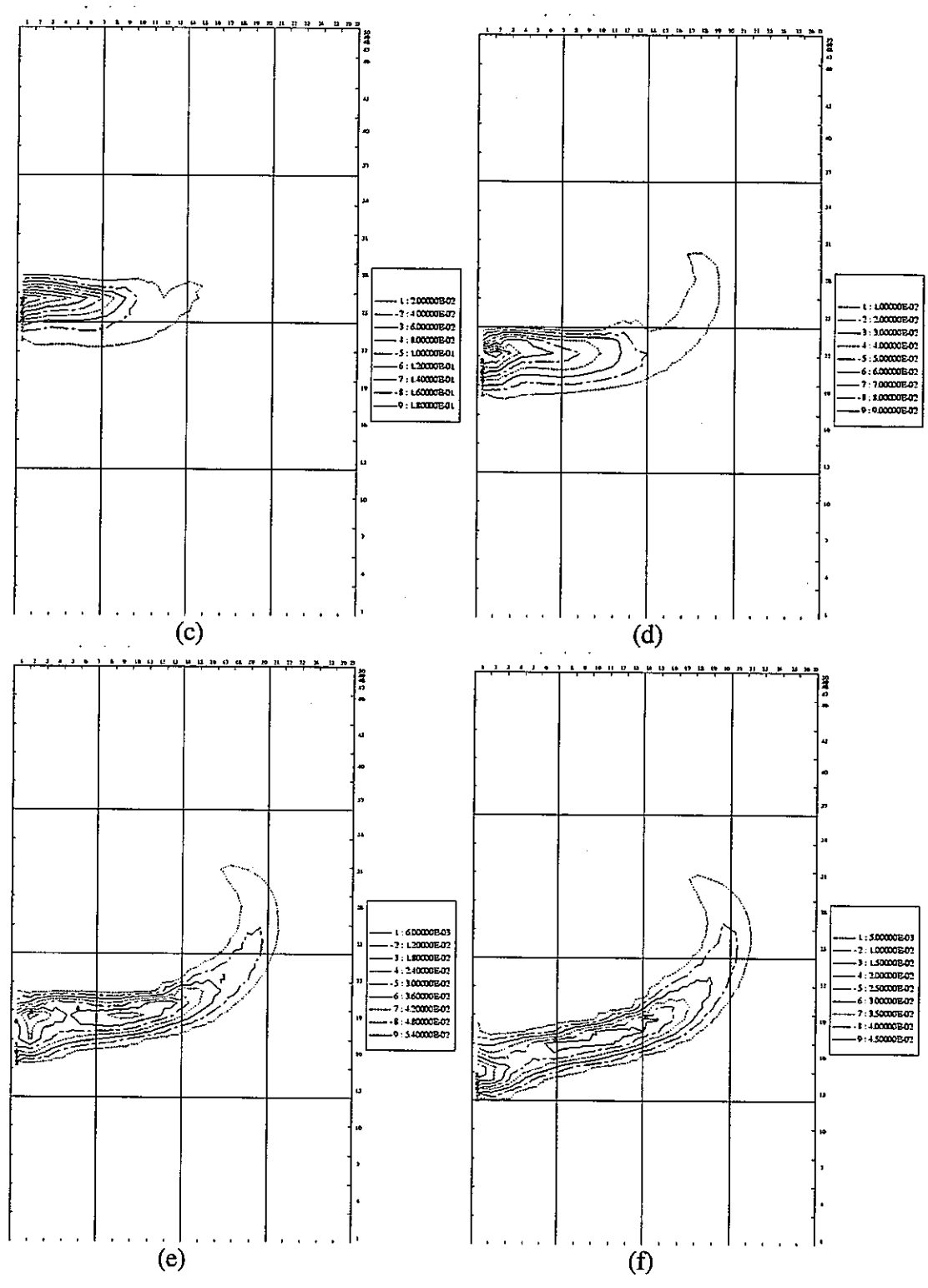

Fig. 20. Contour graphs of the volume fraction of the sphere cloud in Q-12, plotted at time of 0.53, 0.586, 0.642, 0.698, 0.754 and 0.81 second from (a) through (f).

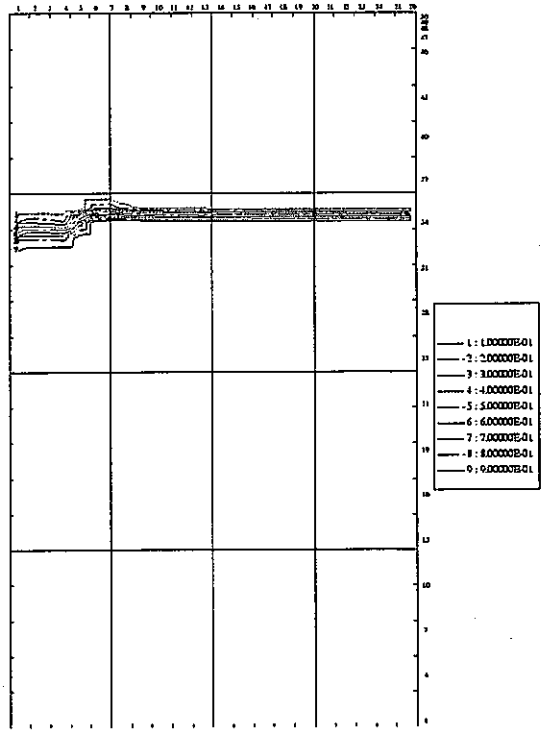

(a)

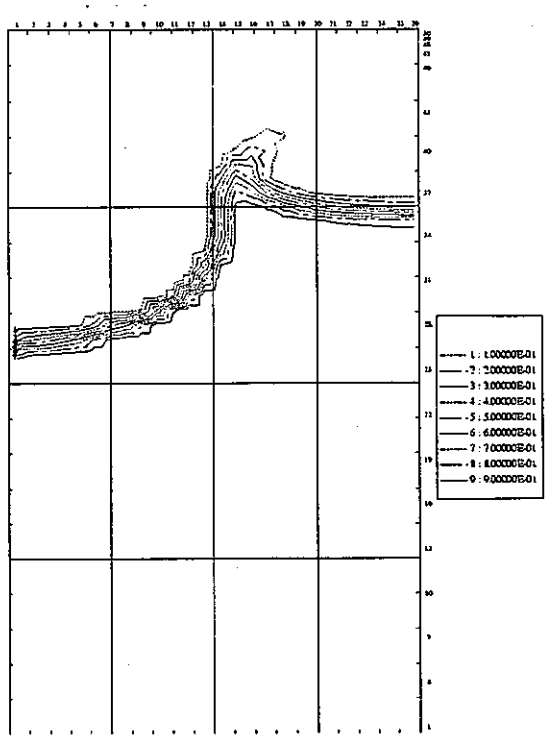

(b)

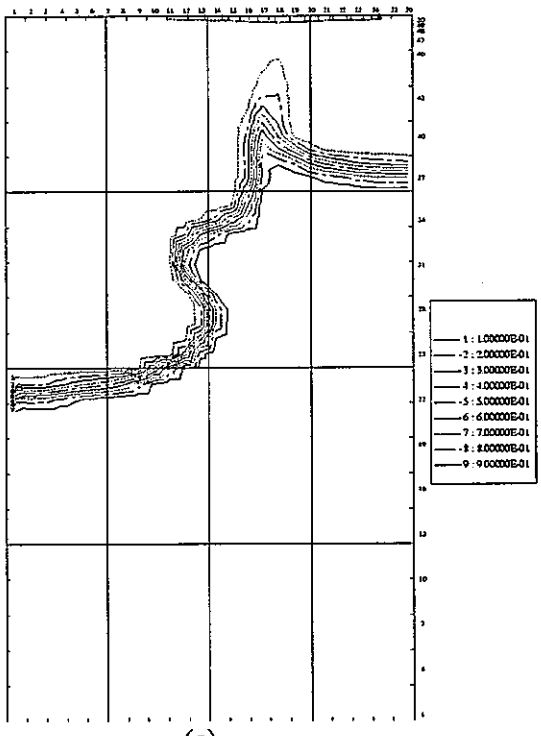

(c)

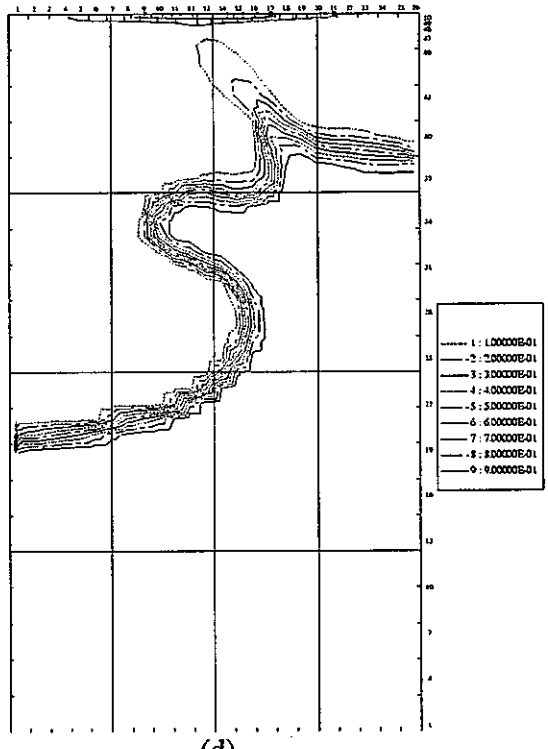

(d)

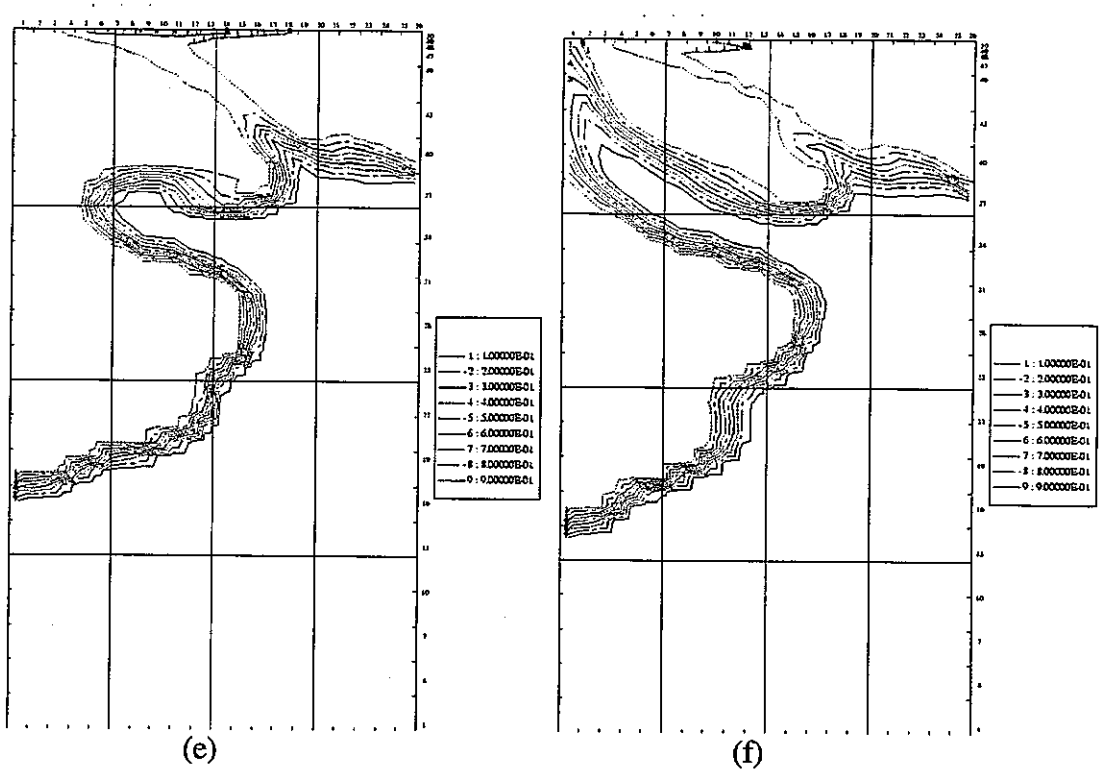

Fig. 21. Contour graphs of the volume fraction of water in Q-12, plotted at time of 0.53, 0.586, 0.642, 0.698, 0.754 and 0.81 second from (a) through (f).

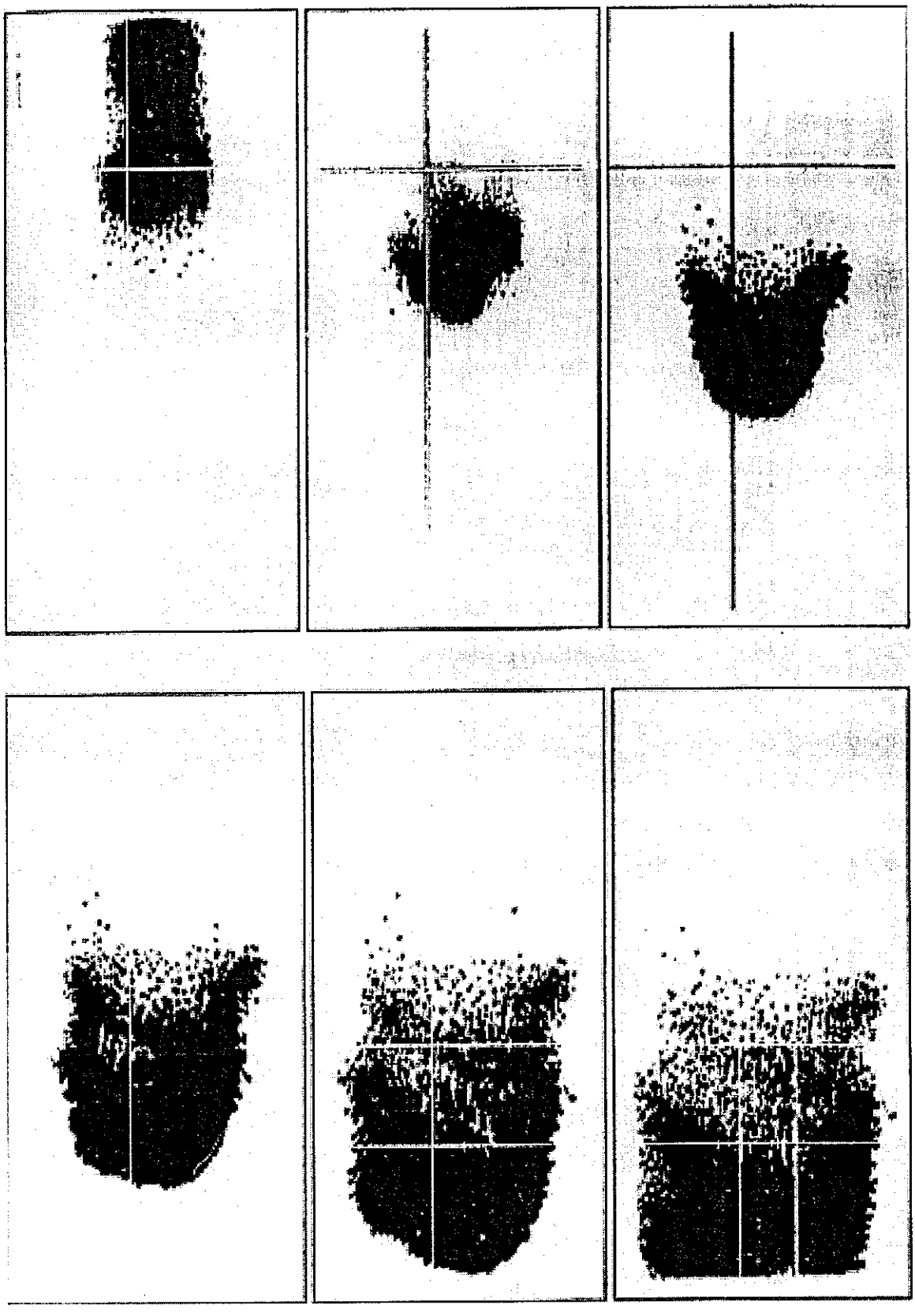

Fig. 22. Images of molybdenum sphere cloud falling in water in Q-12

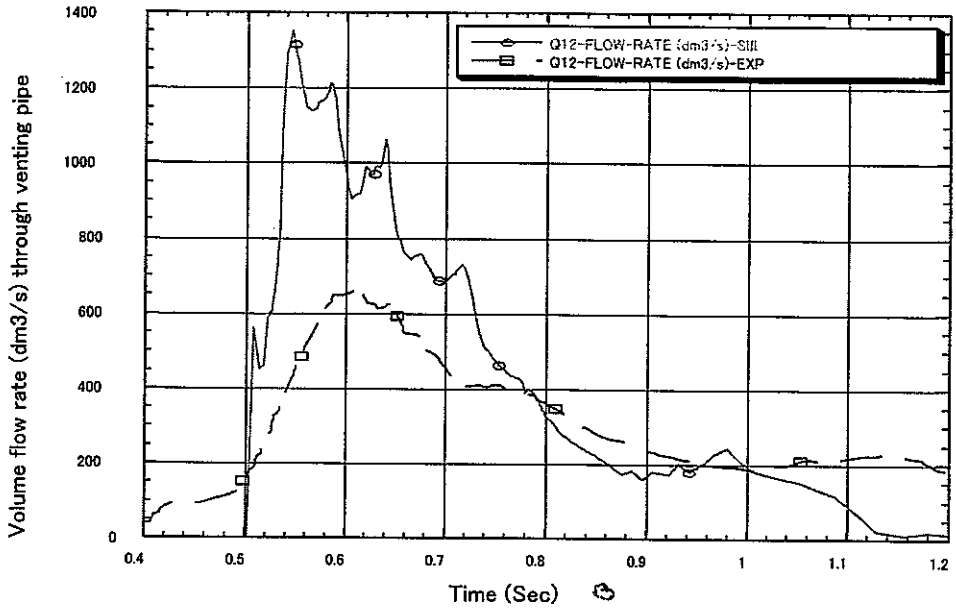

Fig. 23. Volume flow rate through venting pipe in Q-12

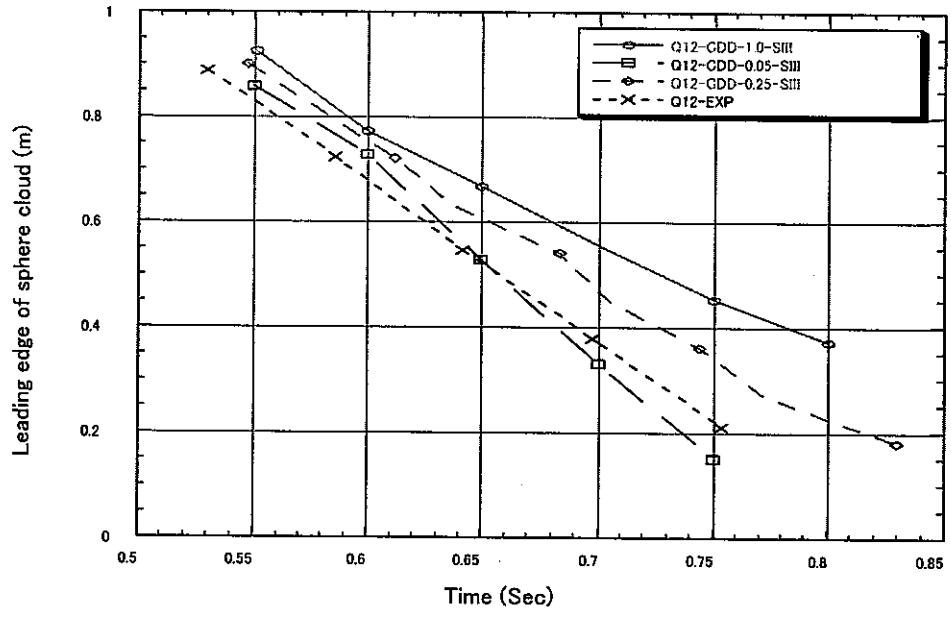

Fig. 24. Evolution of the leading edge of the sphere cloud in cases with different drag coefficient multiplier CDD and CCD of 0.05, 0.25 and 1.0 in Q-12.

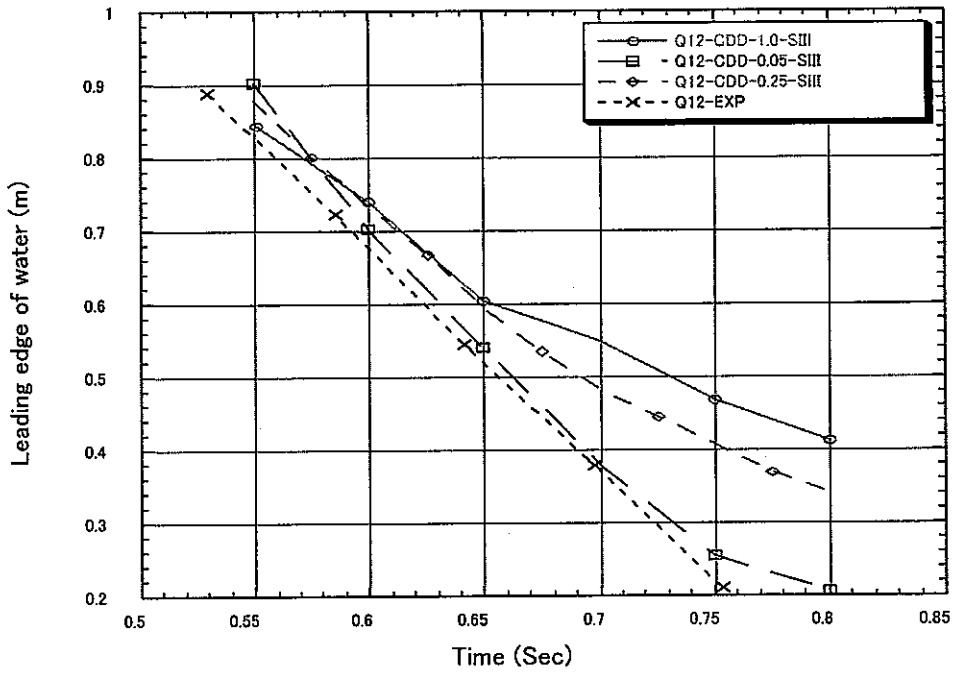

Fig. 25. Evolution of the leading edge of water in cases with different drag coefficient multiplier CDD and CCD of 0.05, 0.25 and 1.0 in Q-12.

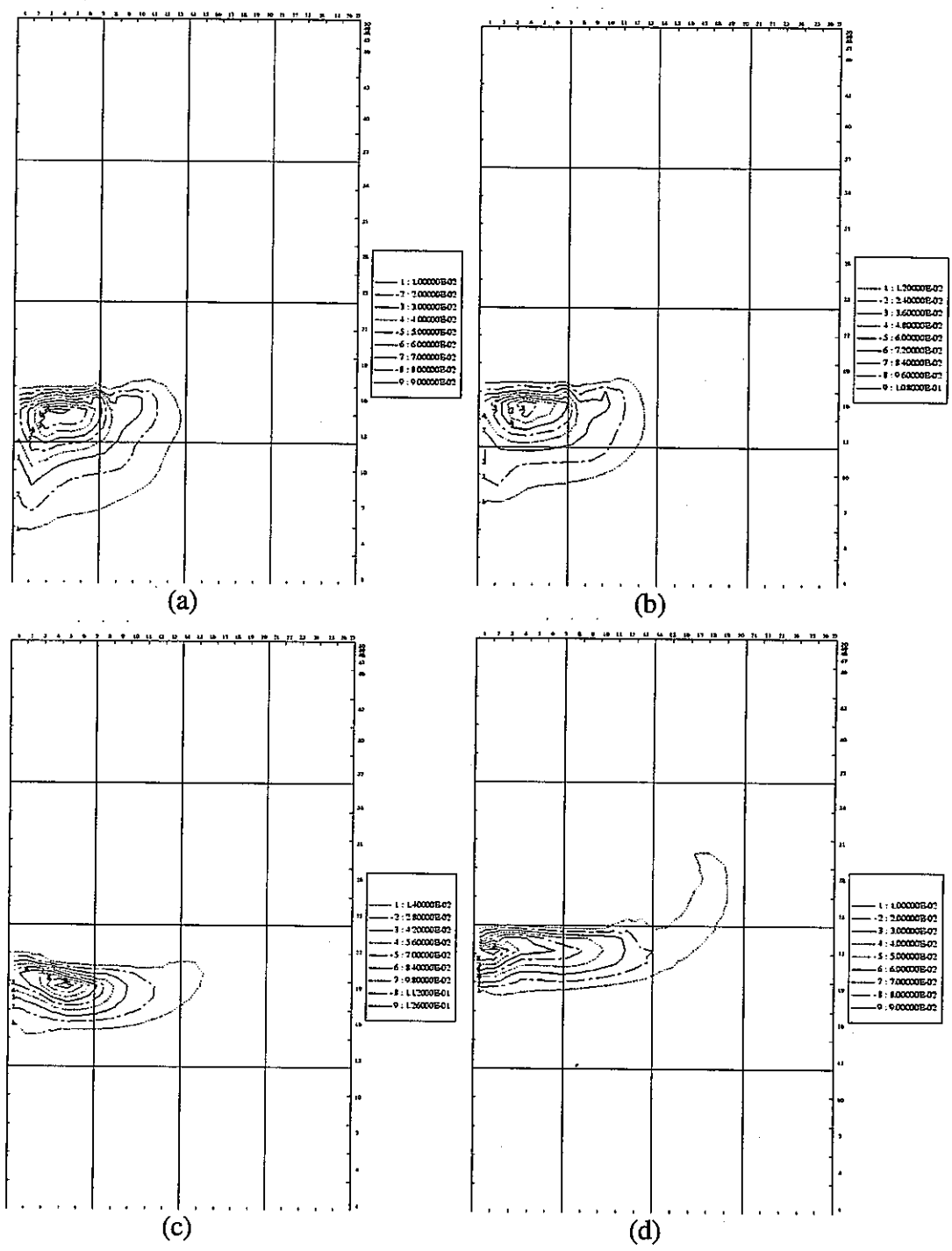

Fig. 26. Contour graphs of the volume fraction of the sphere cloud in Q-12, plotted at time of 0.698 second for the cases with drag coefficient multiplier of 0.025, 0.05, 0.25 and 1.0 from (a) through (d).

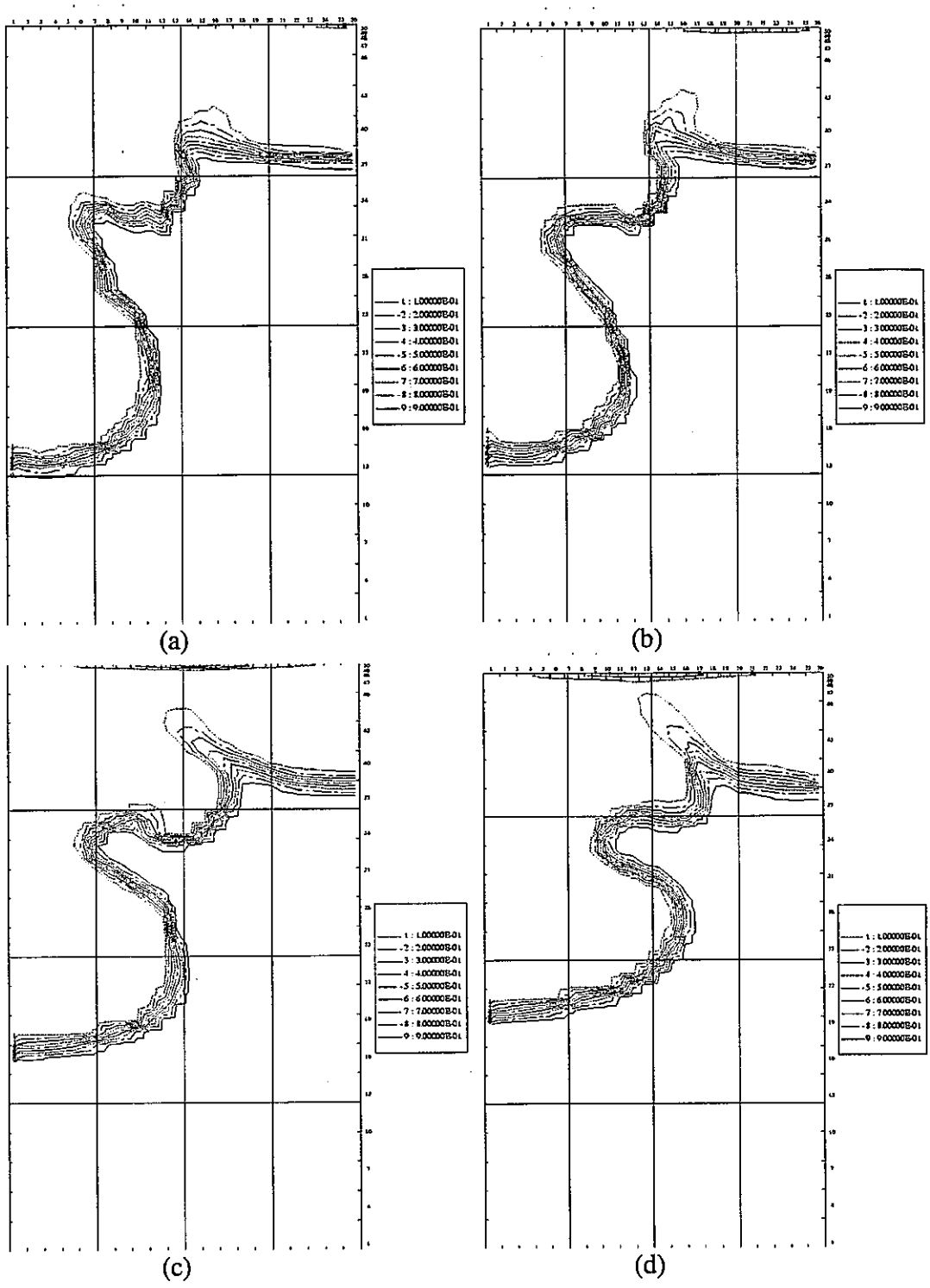

Fig. 27. Contour graphs of the volume fraction of water in Q-12, plotted at time of 0.698 second for the cases with drag coefficient multiplier of 0.025, 0.05, 0.25 and 1.0 from (a) through (d).

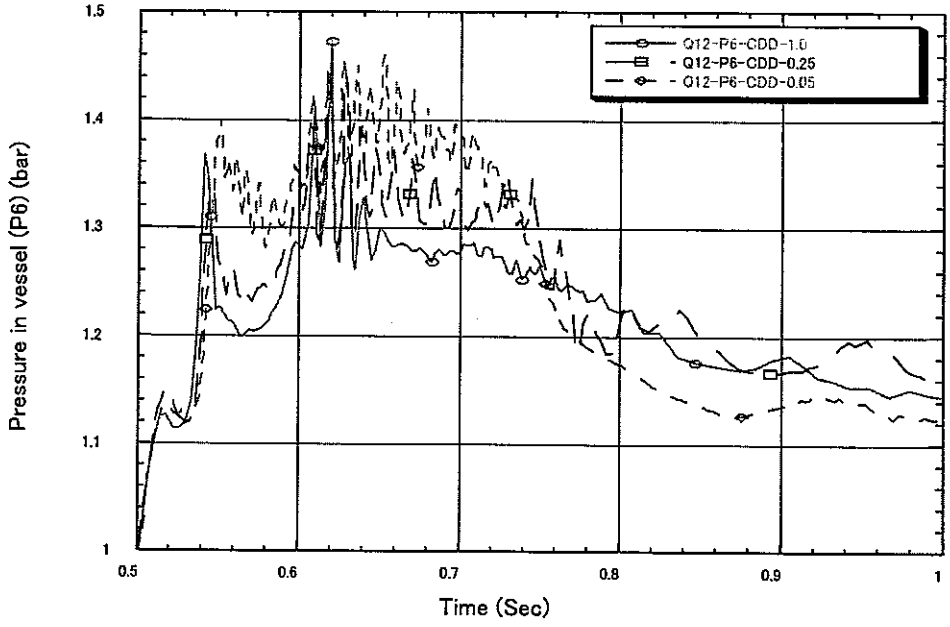

Fig. 28. Pressure transient in the vessel at position of P6 in the cases of Q-12 with different multiplier of drag coefficient.

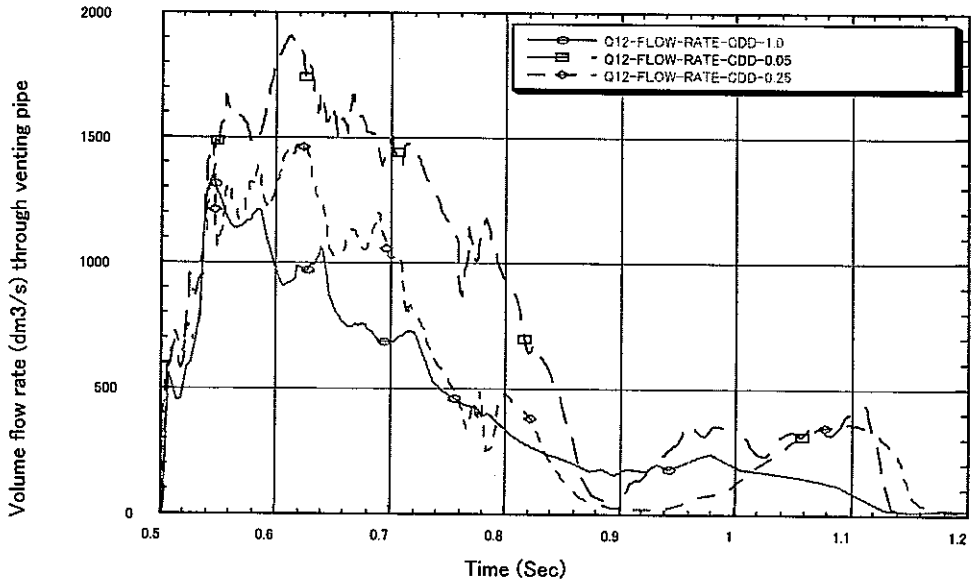

Fig. 29. Gas flow rate through venting pipe in the cases of Q-12 with different multiplier of drag coefficient.

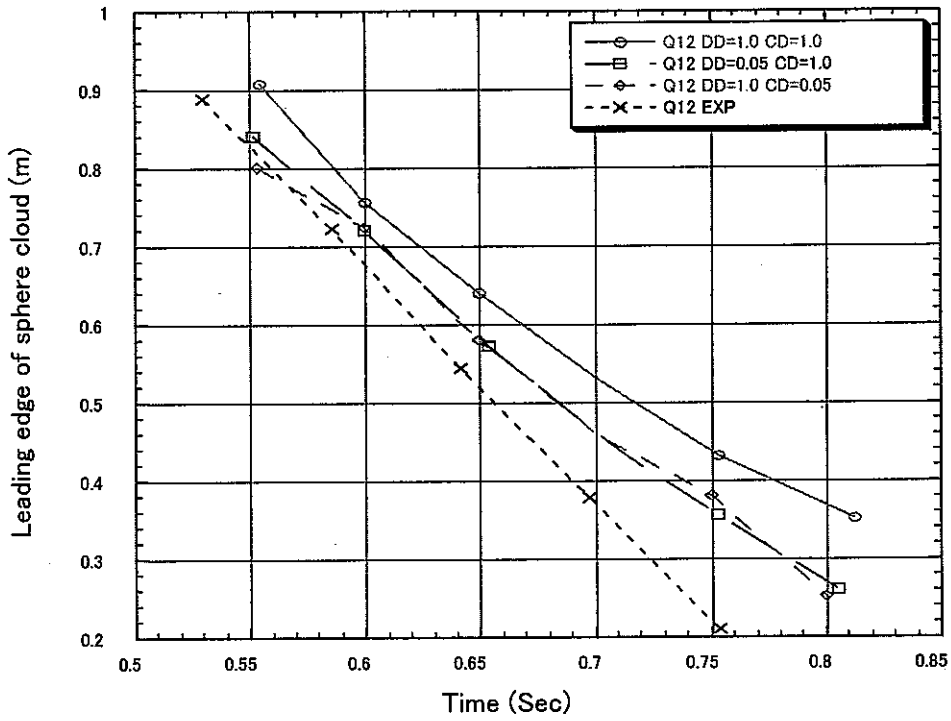

Fig. 30. Evolution of the leading edge of the sphere cloud in cases with different combination of drag coefficient multipliers in Q-12.

Appendix A Input Listing

Input file of Q-08

```
START Q08
 QUEOS 08 - CCD = 1.0,CDD = 1.0
-------------------------------------------------------
###### BLOCK 2 #####
 &XCNTL
  ALGOPT(1)   = 100*0,
  ALGOPT(1)   =    4,  0,  1,  1,  1,  0,  0,  0,  1,
1,
  ALGOPT(11)  =    1,  0,  0,  1,  1,  1,  1,  1,  1,
0,
  ALGOPT(24)  =    2,  1,
  ALGOPT(31)  =    0,  0,  1,  0,  0,  0,  0,  0,  0,
0,
ALGOPT(61)  =    0,  0,  0,  0,  1,  0,  0,  0,  0,
0,

  EOSOPT(1)   =    0,  0,  0,  0,  0,  0,  0,  0,  0,
0,

  HTCOPT(1)   = 100*0,
  HTCOPT(1)   =    0,  0,  1,  0,  0,  0,  0,  0,  0,
0,
  HTCOPT(7)   =    0,
  HTCOPT(10)  =    1,
  HTCOPT(11)  =    2,  0,  1,  1,  0,  0,  0,  0,  0,
0,

  IFAOPT(1)   = 100*0,
  IFAOPT(1)   =    1,  0,  0,  0,  0,  0,  0,  0,  0,
0,
  IFAOPT(20)  =    0,  0,  0,  0,  0,  0,  0,  0,  0,
0,

  HMTOPT(1)   = 100*0,
  HMTOPT(7)   =   51,  0,  0,
  HMTOPT(11)  =    0,  0,  0,  0,  0,  2,  0,  0,  0,
0,
  HMTOPT(51)  =    2,  2,
  HMTOPT(61)  =    1,

  EDTOPT(1)   = 100*0,
  EDTOPT(1)   =    1,  0,  0,  1,  0,  2,
  EDTOPT(11)  =    1,  0,  0,  0,  0,  0,  0,  0,  0,
0,

 &END

###### BLOCK 3 ###### QUEOS MESH  WITH WALLS  -----
---------------
 &XMSH
  IB          =    27,
  JB          =    50,
  NREG        =    10,
  DRINP(1)    =  23*0.015,2*0.018,0.0103,0.0103,
  DZINP(1)    =
34*0.03,2*0.028,6*0.028,1*0.016,3*0.032,1*0.024,3*0.0116,
 &END

###### BLOCK 4 ######
 &XTME
  TSTART      =    0.50,
  TWFIN       =    1.200,
  TCPU        =    800000.00,
  DTSTRT      =    4.0D-05,
  DTMIN       =    1.0D-07,
  DTMAX       =    4.0D-05,
  NDT0        =    1,
 &END

######BLOCK 5 ######   ..... LIQUID COLUMN + GAS
 SPACE
  &XRGN
   RGNAMB = 'WATER -R1',
   LRGN=1, ILB=1,IUB=26,JLB=1,JUB=4,
   ALMINB(3) = 1.0000,
   TLMINB(3) = 370.50,
   PSFINB    = 1.0000D+05,
   TGINB     = 370.50,
   RLM0IB(1) =6*0.001, RGB0IB=0.001, XENRIB(1)=6*1.0,
   RLM0IB(4) =0.0021, RLMINB(4)=0.0021,
RLMAXB(4)=0.0021,
   RLM0IB(3) =0.0001, RLMINB(3)=0.000001,
RLMAXB(3)=0.0001,
  &END
  &XRGN
   RGNAMB = 'WATER -R2',
   LRGN=2, ILB=1,IUB=26,JLB=5,JUB=34,
   ALMINB(3) = 1.0000,
   TLMINB(3) = 370.5,
   PSFINB    = 1.0000D+05,
   TGINB     = 370.50,
   RLM0IB(1) =6*0.001, RGB0IB=0.001, XENRIB(1)=6*1.0,
   RLM0IB(4) =0.0021, RLMINB(4)=0.0021,
RLMAXB(4)=0.0021,
   RLM0IB(3) =0.0001, RLMINB(3)=0.000001,
RLMAXB(3)=0.0001,
  &END
  &XRGN
   RGNAMB = 'GAS    R3'
   LRGN=3, ILB=1,IUB=6,JLB=35,JUB=36,
   ALMINB(3) = 0.0030,
   TLMINB(3) = 370.5,
   PGMINB(3) = 0.000100D+05,
   TGINB     = 370.50,
   PG4INB    = 0.9999D+5,
   RLM0IB(1) =6*0.001, RGB0IB=0.001, XENRIB(1)=6*1.0,
   RLM0IB(4) =0.0021, RLMINB(4)=0.0021,
RLMAXB(4)=0.0021,
   RLM0IB(3) =0.0001, RLMINB(3)=0.000001,
RLMAXB(3)=0.0001,
  &END
  &XRGN
   RGNAMB = 'PARTICLES  -R4'
   LRGN=4, ILB=1,IUB=6,JLB=37,JUB=46,
   ALMINB(4) = 1.0D-15,
   TLMINB(4) = 300.0,
   ALMINB(3) = 0.0030,
   TLMINB(3) = 370.5,
   PGMINB(3) = 1.0D+01,
   PG4INB    = 0.9999D+5,
   TGINB     = 370.5,
   RLM0IB(1) =6*0.001, RGB0IB=0.001, XENRIB(1)=6*1.0,
   RLM0IB(4) =0.0021, RLMINB(4)=0.0021,
RLMAXB(4)=0.0021,
   RLM0IB(3) =0.0001, RLMINB(3)=0.000001,
RLMAXB(3)=0.0001,
  &END
  &XRGN
   RGNAMB = 'GAS    R5'
   LRGN=5, ILB=7,IUB=26,JLB=35,JUB=46,
   ALMINB(3) = 0.0030,
   TLMINB(3) = 370.5,
   PGMINB(3) = 1.0000D+01,
   PG4INB    = 0.9999D+5,
   TGINB     = 370.50,
   RLM0IB(1) =6*0.001, RGB0IB=0.001, XENRIB(1)=6*1.0,
   RLM0IB(4) =0.0021, RLMINB(4)=0.0021,
RLMAXB(4)=0.0021,
   RLM0IB(3) =0.0001, RLMINB(3)=0.000001,
RLMAXB(3)=0.0001,
  &END
  &XRGN
   RGNAMB = 'GAS    R6'
   LRGN=6, ILB=1,IUB=26,JLB=47,JUB=47,
   ALMINB(3) = 0.0030,
```

```
  TLMINB(3) = 370.5,
  PGMINB(3) = 1.0000D+01,
  PG4INB    = 0.9991D+5,
  TGINB     = 370.50,
  RLM0IB(1) =6*0.001, RGB0IB=0.001, XENRIB(1)=6*1.0,
  RLM0IB(4) =0.0021, RLMINB(4)=0.0021,
RLMAXB(4)=0.0021,
  RLM0IB(3) =0.0001, RLMINB(3)=0.000001,
RLMAXB(3)=0.0001,
 &END
 &XRGN
  RGNAMB = 'GAS     R7'
  LRGN=7, ILB=1,IUB=26,JLB=48,JUB=50,
  ALMINB(3) = 0.0030,
  TLMINB(3) = 370.5,
  PGMINB(3) = 1.0000D+01,
  PG4INB    = 0.9999D+5,
  TGINB     = 370.50,
  RLM0IB(1) =6*0.001, RGB0IB=0.001, XENRIB(1)=6*1.0,
  RLM0IB(4) =0.0021, RLMINB(4)=0.0021,
RLMAXB(4)=0.0021,
  RLM0IB(3) =0.0001, RLMINB(3)=0.000001,
RLMAXB(3)=0.0001,
 &END
 &XRGN
  RGNAMB = 'STRUCT-R8',
  LRGN=8, ILB=27,IUB=27,JLB=1,JUB=4,
  ALMINB(3) = 0.4500,
  TLMINB(3) = 365.0,
  PSFINB    = 1.0000D+05,
  TGINB     = 365.00,
  ARCWIB    = 97.00,
  ASMINB(7) = 0.05,
  ASMINB(8) = 0.45,
  TSINB(7) = 365.00,
  TSINB(8) = 365.00,
  RLM0IB(1) =6*0.001, RGB0IB=0.001, XENRIB(1)=6*1.0,
  RLM0IB(4) =0.0021, RLMINB(4)=0.0021,
RLMAXB(4)=0.0021,
  RLM0IB(3) =0.0001, RLMINB(3)=0.000001,
RLMAXB(3)=0.0001,
 &END
 &XRGN
  RGNAMB = 'STRUCT-R9',
  LRGN=9, ILB=27,IUB=27,JLB=5,JUB=34,
  ALMINB(3) = 0.4500,
  TLMINB(3) = 370.5,
  PSFINB    = 1.0000D+05,
  TGINB     = 370.50,
  ARCWIB    = 97.00,
  ASMINB(7) = 0.05,
  ASMINB(8) = 0.45,
  TSINB(7) = 370.50,
  TSINB(8) = 370.50,
  RLM0IB(1) =6*0.001, RGB0IB=0.001, XENRIB(1)=6*1.0,
  RLM0IB(4) =0.0021, RLMINB(4)=0.0021,
RLMAXB(4)=0.0021,
  RLM0IB(3) =0.0001, RLMINB(3)=0.000001,
RLMAXB(3)=0.0001,
 &END
 &XRGN
  RGNAMB = 'STRUCT-R10'
  LRGN=10, ILB=27,IUB=27,JLB=35,JUB=50,
  ALMINB(3) = 0.0020,
  TLMINB(3) = 370.50,
  TGINB     = 370.50,
  PSFINB    = 1.0D+5,
  ARCWIB    = 97.00,
  ASMINB(7) = 0.05,
  ASMINB(8) = 0.45,
  TSINB(7) = 370.500,
  TSINB(8) = 370.500,
  RLM0IB(1) =6*0.001, RGB0IB=0.001, XENRIB(1)=6*1.0,
  RLM0IB(4) =0.0021, RLMINB(4)=0.0021,
RLMAXB(4)=0.0021,
  RLM0IB(3) =0.0001, RLMINB(3)=0.000001,
RLMAXB(3)=0.0001,
 &END

######BLOCK 6 ######
 &XCWD

  VC(1,37,1) =  -5.00,
  VC(2,37,1) =  -5.00,
  VC(3,37,1) =  -5.00,
  VC(4,37,1) =  -5.00,
  VC(5,37,1) =   0.00,
  VC(6,37,1) =   0.00,

  VC(1,38,1) =  -4.90,
  VC(2,38,1) =  -4.90,
  VC(3,38,1) =  -4.90,
  VC(4,38,1) =  -4.90,
  VC(5,38,1) =   0.00,
  VC(6,38,1) =   0.00,

  VC(1,39,1) =  -4.80,
  VC(2,39,1) =  -4.80,
  VC(3,39,1) =  -4.80,
  VC(4,39,1) =  -4.80,
  VC(5,39,1) =  -4.80,
  VC(6,39,1) =   0.00,

  VC(1,40,1) =  -4.70,
  VC(2,40,1) =  -4.70,
  VC(3,40,1) =  -4.70,
  VC(4,40,1) =  -4.70,
  VC(5,40,1) =  -4.70,
  VC(6,40,1) =  -4.70,

  VC(1,41,1) =  -4.60,
  VC(2,41,1) =  -4.60,
  VC(3,41,1) =  -4.60,
  VC(4,41,1) =  -4.60,
  VC(5,41,1) =  -4.60,
  VC(6,41,1) =  -4.60,

  VC(1,42,1) =  -4.50,
  VC(2,42,1) =  -4.50,
  VC(3,42,1) =  -4.50,
  VC(4,42,1) =  -4.50,
  VC(5,42,1) =  -4.50,
  VC(6,42,1) =  -4.50,

  VC(1,43,1) =  -4.40,
  VC(2,43,1) =  -4.40,
  VC(3,43,1) =  -4.40,
  VC(4,43,1) =  -4.40,
  VC(5,43,1) =  -4.40,
  VC(6,43,1) =  -4.40,

  VC(1,44,1) =  -4.30,
  VC(2,44,1) =  -4.30,
  VC(3,44,1) =  -4.30,
  VC(4,44,1) =  -4.30,
  VC(5,44,1) =  -4.30,
  VC(6,44,1) =  -4.30,

  VC(1,45,1) =  -4.20,
  VC(2,45,1) =  -4.20,
  VC(3,45,1) =  -4.20,
  VC(4,45,1) =  -4.20,
  VC(5,45,1) =  -4.20,
  VC(6,45,1) =  -4.20,

  VC(1,46,1) =  -4.10,
  VC(2,46,1) =  -4.10,
  VC(3,46,1) =  -4.10,
  VC(4,46,1) =  -4.10,
  VC(5,46,1) =  -4.10,
```

```
 VC(6,46,1) =   0.00,


 ALC(1,37,4) =  0.170,
 ALC(2,37,4) =  0.170,
 ALC(3,37,4) =  0.170,
 ALC(4,37,4) =  0.170,
 ALC(5,37,4) =  1.0D-15,
 ALC(6,37,4) =  1.0D-15,

 ALC(1,38,4) =  0.170,
 ALC(2,38,4) =  0.170,
 ALC(3,38,4) =  0.170,
 ALC(4,38,4) =  0.170,
 ALC(5,38,4) =  1.0D-15,
 ALC(6,38,4) =  1.0D-15,

 ALC(1,39,4) =  0.170,
 ALC(2,39,4) =  0.170,
 ALC(3,39,4) =  0.170,
 ALC(4,39,4) =  0.170,
 ALC(5,39,4) =  0.170,
 ALC(6,39,4) =  1.0D-15,

 ALC(1,40,4) =  0.170,
 ALC(2,40,4) =  0.170,
 ALC(3,40,4) =  0.170,
 ALC(4,40,4) =  0.170,
 ALC(5,40,4) =  0.170,
 ALC(6,40,4) =  0.170,

 ALC(1,41,4) =  0.170,
 ALC(2,41,4) =  0.170,
 ALC(3,41,4) =  0.170,
 ALC(4,41,4) =  0.170,
 ALC(5,41,4) =  0.170,
 ALC(6,41,4) =  0.170,

 ALC(1,42,4) =  0.170,
 ALC(2,42,4) =  0.170,
 ALC(3,42,4) =  0.170,
 ALC(4,42,4) =  0.170,
 ALC(5,42,4) =  0.170,
 ALC(6,42,4) =  0.170,

 ALC(1,43,4) =  0.170,
 ALC(2,43,4) =  0.170,
 ALC(3,43,4) =  0.170,
 ALC(4,43,4) =  0.170,
 ALC(5,43,4) =  0.170,
 ALC(6,43,4) =  0.170,

 ALC(1,44,4) =  0.170,
 ALC(2,44,4) =  0.170,
 ALC(3,44,4) =  0.170,
 ALC(4,44,4) =  0.170,
 ALC(5,44,4) =  0.170,
 ALC(6,44,4) =  0.170,

 ALC(1,45,4) =  0.170,
 ALC(2,45,4) =  0.170,
 ALC(3,45,4) =  0.170,
 ALC(4,45,4) =  0.170,
 ALC(5,45,4) =  0.170,
 ALC(6,45,4) =  0.170,

 ALC(1,46,4) =  0.170,
 ALC(2,46,4) =  0.170,
 ALC(3,46,4) =  0.170,
 ALC(4,46,4) =  0.170,
 ALC(5,46,4) =  0.170,
 ALC(6,46,4) =  1.0D-15,

 TLC(1,1,4) = 1350*300.0,
```

```
  &END

 ######BLOCK 7 ######
  &XEDT
   PRTC=5000,PPFC=100,DMPC=999991,BSFC=100,
   DTEOS(1,1)=300,50,3900,
   NPRINT(1)=2,
   NPAGE= 5,
   LPRGN(10) = 1,0,0,1,
   LPRGN(17) = 1,
   LPRGN(30) = 1,1,0,0,1,1,
   SN(1)='ALPLK1','ALPLK2','ALPLK3',

 'ALPLK4','ALPLK5','ALPLK6','ALPGK','ALPGE','PK','IRGMK',
        'TLK1','TLK2','TLK3','TLK4','TLK5','TLK6','TGK',
        'VK1','VK2','VK3','UK1','UK2','UK3',
        'RGBK','CPK','DPK',
        'RBGK1','RBGK2','RBGK3','RBGK4','RBGK5',

 'RBLK1','RBLK2','RBLK3','RBLK4','RBLK5','RBLK6','RBLK7','
 RBLK8',
        'RBLK9','RBLK10',
        'ALPGEK',
        'TSAT1','TSAT2','TSAT3',
        'PGMK1','PGMK2','PGMK3','PGMK4',

  &END

 ###### BLOCK 8 ######
  &XEOS
    ISAE(2,1)    =   1,
    IMRK(2,1)    =   0,
    ISPN(2,1)    =   0,
   BETA(2,1)     =-1.00000D+00,
   ESOLUS(2,1)   = 1.56000D+06,
   ELIQUS(2,1)   = 1.56520D+06,
   CVG(2,1)      = 5.20000D+02,
   TCRT(2,1)     = 8.50000D+03,
   RUGM(2,1)     = 8.66636D+01,
   WM(2,1)       = 9.59400D+01,
   TSOLUS(2,1)   = 3.00000D+03,
   TLIQUS(2,1)   = 3.01000D+03,
   ELIQG(2,1)    = 6.75606D+06,
   PCRT(2,1)     = 1.60651D+10,
   ELIQGD(2,1)   = 6.75606D+06,
   VSOLUS(2,1)   = 9.80392D-05,
   VLIQUS(2,1)   = 9.80392D-05,
   ECRT(2,1)     = 4.42000D+06,
   ROCRT(2,1)    = 1.02000D+04,
   PSMIN(2,1)    = 1.85005D-05,
   DTDPS(2,1)    = 0.00000D+00,
   DVDPS(2,1)    =-1.53787D-15,
   DTDPC(2,1)    = 0.00000D+00,
   AS(1,2,1)     = 1.00000D+00, 0.00000D+00, 0.00000D+00,
   BS(1,2,1)     = 0.00000D+00, 0.00000D+00, 0.00000D+00,
   AL(1,2,1)     = 1.00000D+00, 0.00000D+00, 0.00000D+00,
                   2.82392D+00, 0.00000D+00, 0.00000D+00,
   BL(1,2,1)     = 3.09007D+01, 0.00000D+00,-6.29066D+04,
                   0.00000D+00,
   CL(1,2,1)     = 0.00000D+00, 0.00000D+00, 0.00000D+00,
                   0.00000D+00,
   DL(1,2,1)     = 0.00000D+00, 0.00000D+00, 0.00000D+00,
                   2.82392D+00, 0.00000D+00, 0.00000D+00,
   FL(1,2,1)     = 0.00000D+00, 0.00000D+00, 0.00000D+00,
                   0.00000D+00, 0.00000D+00, 0.00000D+00,
   DG(1,2,1)     = 0.00000D+00, 0.00000D+00,
   FG(1,2,1)     = 0.00000D+00, 0.00000D+00, 0.00000D+00,
                   0.00000D+00,
   AG(1,2,1)     = 0.00000D+00, 0.00000D+00, 1.00000D+00,
                   0.00000D+00,
   BG(1,2,1)     = 3.29486D-12, 6.29066D+04, 0.00000D+00,
                   0.00000D+00, 0.00000D+00, 0.00000D+00,
   CG(1,2,1)     = 5.20000D+02, 0.00000D+00, 0.00000D+00,
                   1.00000D+00, 0.00000D+00, 0.00000D+00,
   ASAT(1,2,1)   = 4.91215D-04,-1.58966D-05, 0.00000D+00,
```

```
              0.00000D+00,
 BSAT(1,2,1)  = 0.00000D+00, 0.00000D+00, 0.00000D+00,
              1.00000D+00, 0.00000D+00, 0.00000D+00,
 CSAT(1,2,1)  = 5.20000D+02, 0.00000D+00, 0.00000D+00,
              1.00000D+00, 0.00000D+00, 0.00000D+00,
 &END

###### BLOCK 9 ###### --- ORIFICE
 &XMXF
  CDD = 1.0,
  CCD = 1.0,
  CORFZN(1,54) =    2.27,
  CORFZN(2,54) =    2.27,
  CORFZN(3,54) =    2.27,
  CORFZN(4,54) =    2.27,

 &END

###### BLOCK 10 ######
 &XIFA
  DHPOOL  =  1.00,
  RLMIN(1)=0.0021, RLMAX(1)=0.0021,
  RLMIN(4)=0.0021, RLMAX(4)=0.0021,
  CLL(1,3)=1.00,
  CLL(4,3)=1.00,
 &END

###### BLOCK 11 ######
 &XHTC
  HFCLP(1,3) =  5.10000D-01,
  HFCLP(2,3) =  5.00000D-01,
  HFCLP(3,3) =  4.00000D-01,
  HFCLP(4,3) =  1.50000D-02,
  HFCLP(5,3) =  3.33333D-01,

  HNCLP(1,3) =  5.00000D-01,
  HNCLP(2,3) =  2.50000D-01,
  HNCLP(3,3) =  1.18000D-00,

  HFCLS(1,3) =  2.30000D-02,
  HFCLS(2,3) =  8.00000D-01,
  HFCLS(3,3) =  3.00000D-01,

  FILMIN     =  1.00000D-04,
  CMFB       =  0.64,

  HCDGS      =  5.0,
  HCDLAS(1)  =  3*2.0,

 &END

###### BLOCK 12 ######
 &XBND
  NBC        =   0,
  LBCSET     =   29*0,1450*0,0,4*1,24*0,
 &END

 &XBND
  NBC        =   1,
  LBCS       =   2,
  LBCP       =   4,
  PTAB(1)    =   1.00D5, 1.00D5, 1.00D5, 1.00D5,
  PTME(1)    =  -0.500,  0.000,  0.5000, 2.0000,
 &END

###### BLOCK 13 ###### AKPS = 88-142 W/MK

 &XTPP
  AKPL(1,2,1)  = 6.60000D+01, 0.00000D+00, 0.00000D+00,
  AKPS(1,2,1)  = 6.60000D+01, 0.00000D+00, 0.00000D+00,
               0.00000D+00, 0.00000D+00,

  EMSVS(2,1)   =  0.3,
  EMSVL(2,1)   =  0.3,
  EMSVL(2,3)   =  0.95,
 &END

###### BLOCK 15 ######
 &XHMT
  FMTLG=2.0D-4,
  PHI   = 0.01,
  MIVC  =290,
  IVCHLG=260,
  FTSTL = 0.6,
  FRG=0.2,
  FTG=0.3,
  FTSTH = 0.95,
 &END
###### BLOCK 17 ######
 &XMSC
  COURTN      =  0.3,
  OPTPIT      =  9,
  MPIT        =  900,
  MAXITC      =  300,
  EPSVEL      =  1.0D-04,
  EPSP        =  1.0D-01,
  EPSRO       =  1.0D-04,
  EPST        =  1.0,
  EPSPCV      =  1.0D-04,
 &END
###### BLOCK 18 ######
 &XERG
  REGN        =   1,
  REGC(1,1)   =   1,
  REGC(2,1)   =   1,
  REGC(3,1)   =  27,
  REGC(4,1)   =  50,
  MATEOS(1,1) =   2,
  MATEOS(2,1) =   2,
  MATEOS(3,1) =   2,
  MATEOS(4,1) =   2,
  MATEOS(5,1) =   2,
 &END
```

Input file of Q-12

```
START   Q12
 QUEOS 12 - CCD = 1.0   CDD = 1.0
-------------------------------------------------------------
###### BLOCK 2 #####
 &XCNTL
  ALGOPT(1)    = 100*0,
  ALGOPT(1)    =      4,   0,   1,   1,   1,   0,   0,
0,   1,   1,
  ALGOPT(11)   =      1,   0,   0,   1,   1,   1,   1,
1,   1,   0,
  ALGOPT(24)   =      2,   1,
  ALGOPT(31)   =      0,   0,   1,   0,   0,   0,   0,
0,   0,   0,
  ALGOPT(61)   =      0,   0,   0,   0,   1,   0,   0,
0,   0,   0,

  EOSOPT(1)    =      0,   0,   0,   0,   0,   0,   0,   0,
0,   0,

  HTCOPT(1)    = 100*0,
  HTCOPT(1)    =      0,   0,   1,   0,   0,   0,   0,
0,   0,   0,
  HTCOPT(7)    =      0,
  HTCOPT(10)   =      1,
  HTCOPT(11)   =      2,   0,   1,   1,   0,   0,   0,
0,   0,   0,

  IFAOPT(1)    = 100*0,
  IFAOPT(1)    =      1,   0,   0,   0,   0,   0,   0,   0,
0,   0,
  IFAOPT(20)   =      0,   0,   0,   0,   0,   0,   0,   0,
0,   0,
```

```
   HMTOPT(1)    = 100*0,
   HMTOPT(7)    =       1,  0,   0,
   HMTOPT(11)   =       0,  0,   0,   0,   0,   2,   0,
0,   0,   0,
   HMTOPT(51)   =       2,  2,
   HMTOPT(61)   =       1,

   EDTOPT(1)    = 100*0,
   EDTOPT(1)    =       1,  0,   0,   1,   0,   2,
   EDTOPT(11)   =       1,  0,   0,   0,   0,   0,   0,   0,
0,   0,

 &END

###### BLOCK 3 ###### QUEOS MESH   WITH WALLS   ---
----------
 &XMSH
  IB             =      27,
  JB             =      50,
  NREG           =      10,
  DRINP(1)       =   23*0.015,2*0.018,0.0103,0.0103,
  DZINP(1)       =
34*0.03,2*0.028,6*0.028,1*0.016,3*0.032,1*0.024,3*0.0116,
 &END

###### BLOCK 4 ######
 &XTME
  TSTART         =      0.50,
  TWFIN          =      1.300,
  TCPU           =      800000.00,
  DTSTRT         =      4.0D-05,
  DTMIN          =      1.0D-06,
  DTMAX          =      8.0D-05,
  NDT0           =      1,
 &END

######BLOCK 5 ######     ..... LIQUID COLUMN + GAS
SPACE
 &XRGN
  RGNAMB = 'WATER -R1',
  LRGN=1, ILB=1,IUB=26,JLB=1,JUB=4,
  ALMINB(3) = 1.0000,
  TLMINB(3) = 370.50,
  PSFINB      = 1.0000D+05,
  TGINB       = 370.50,
  RLM0IB(1) =6*0.001, RGB0IB=0.001, XENRIB(1)=6*1.0,
  RLM0IB(4) =0.0021, RLMINB(4)=0.0021,
RLMAXB(4)=0.0021,
  RLM0IB(3) =0.0001, RLMINB(3)=0.000001,
RLMAXB(3)=0.0001,
 &END
 &XRGN
  RGNAMB = 'WATER -R2',
  LRGN=2, ILB=1,IUB=26,JLB=5,JUB=34,
  ALMINB(3) = 1.0000,
  TLMINB(3) = 370.5,
  PSFINB      = 1.0000D+05,
  TGINB       = 370.50,
  RLM0IB(1) =6*0.001, RGB0IB=0.001, XENRIB(1)=6*1.0,
  RLM0IB(4) =0.0021, RLMINB(4)=0.0021,
RLMAXB(4)=0.0021,
  RLM0IB(3) =0.0001, RLMINB(3)=0.000001,
RLMAXB(3)=0.0001,
 &END
 &XRGN
  RGNAMB = 'GAS      R3'
  LRGN=3, ILB=1,IUB=6,JLB=35,JUB=36,
  ALMINB(3) = 0.0010,
  TLMINB(3) = 370.5,
  PGMINB(3) = 1.0000D+03,
  TGINB       = 370.50,
  PG4INB      = 0.99D+5,
  RLM0IB(1) =6*0.001, RGB0IB=0.001, XENRIB(1)=6*1.0,
  RLM0IB(4) =0.0021, RLMINB(4)=0.0021,
RLMAXB(4)=0.0021,
  RLM0IB(3) =0.0001, RLMINB(3)=0.000001,
RLMAXB(3)=0.0001,
 &END
 &XRGN
  RGNAMB = 'PARTICLES   -R4'
  LRGN=4, ILB=1,IUB=6,JLB=37,JUB=46,
  ALMINB(4) = 1.0D-15,
  TLMINB(4) = 2300.0,
  ALMINB(3) = 0.000,
  TLMINB(3) = 370.5,
  PGMINB(3) = 1.0D+03,
  PG4INB      = 0.99D+5,
  TGINB       = 370.5,
  RLM0IB(1) =6*0.001, RGB0IB=0.001, XENRIB(1)=6*1.0,
  RLM0IB(4) =0.0021, RLMINB(4)=0.0021,
RLMAXB(4)=0.0021,
  RLM0IB(3) =0.0001, RLMINB(3)=0.000001,
RLMAXB(3)=0.0001,
 &END
 &XRGN
  RGNAMB = 'GAS      R5'
  LRGN=5, ILB=7,IUB=26,JLB=35,JUB=46,
  ALMINB(3) = 0.0010,
  TLMINB(3) = 370.5,
  PGMINB(3) = 1.0000D+03,
  PG4INB      = 0.99D+5,
  TGINB       = 370.50,
  RLM0IB(1) =6*0.001, RGB0IB=0.001, XENRIB(1)=6*1.0,
  RLM0IB(4) =0.0021, RLMINB(4)=0.0021,
RLMAXB(4)=0.0021,
  RLM0IB(3) =0.0001, RLMINB(3)=0.000001,
RLMAXB(3)=0.0001,
 &END
 &XRGN
  RGNAMB = 'GAS      R6'
  LRGN=6, ILB=1,IUB=26,JLB=47,JUB=47,
  ALMINB(3) = 0.0010,
  TLMINB(3) = 370.5,
  PGMINB(3) = 1.0000D+03,
  PG4INB      = 0.99D+5,
  TGINB       = 370.50,
  RLM0IB(1) =6*0.001, RGB0IB=0.001, XENRIB(1)=6*1.0,
  RLM0IB(4) =0.0021, RLMINB(4)=0.0021,
RLMAXB(4)=0.0021,
  RLM0IB(3) =0.0001, RLMINB(3)=0.000001,
RLMAXB(3)=0.0001,
 &END
 &XRGN
  RGNAMB = 'GAS      R7'
  LRGN=7, ILB=1,IUB=26,JLB=48,JUB=50,
  ALMINB(3) = 0.0010,
  TLMINB(3) = 370.5,
  PGMINB(3) = 1.0000D+03,
  PG4INB      = 0.99D+5,
  TGINB       = 370.50,
  RLM0IB(1) =6*0.001, RGB0IB=0.001, XENRIB(1)=6*1.0,
  RLM0IB(4) =0.0021, RLMINB(4)=0.0021,
RLMAXB(4)=0.0021,
  RLM0IB(3) =0.0001, RLMINB(3)=0.000001,
RLMAXB(3)=0.0001,
 &END
 &XRGN
  RGNAMB = 'STRUCT-R8',
  LRGN=8, ILB=27,IUB=27,JLB=1,JUB=4,
  ALMINB(3) = 0.4500,
  TLMINB(3) = 365.0,
  PSFINB      = 1.0000D+05,
  TGINB       = 365.00,
  ARCWIB      = 97.00,
  ASMINB(7) = 0.05,
  ASMINB(8) = 0.45,
  TSINB(7) = 365.00,
  TSINB(8) = 365.00,
  RLM0IB(1) =6*0.001, RGB0IB=0.001, XENRIB(1)=6*1.0,
  RLM0IB(4) =0.0021, RLMINB(4)=0.0021,
```

```
RLMAXB(4)=0.0021,
  RLM0IB(3) =0.0001, RLMINB(3)=0.000001,
RLMAXB(3)=0.0001,
 &END
 &XRGN
  RGNAMB = 'STRUCT-R9',
  LRGN=9, ILB=27,IUB=27,JLB=5,JUB=34,
  ALMINB(3) = 0.4500,
  TLMINB(3) = 370.5,
  PSFINB      = 1.0000D+05,
  TGINB       = 370.50,
  ARCWIB      = 97.00,
  ASMINB(7) = 0.05,
  ASMINB(8) = 0.45,
  TSINB(7) = 370.50,
  TSINB(8) = 370.50,
  RLM0IB(1) =6*0.001, RGB0IB=0.001, XENRIB(1)=6*1.0,
  RLM0IB(4) =0.0021, RLMINB(4)=0.0021,
RLMAXB(4)=0.0021,
  RLM0IB(3) =0.0001, RLMINB(3)=0.000001,
RLMAXB(3)=0.0001,
 &END
 &XRGN
  RGNAMB = 'STRUCT-R10'
  LRGN=10, ILB=27,IUB=27,JLB=35,JUB=50,
  ALMINB(3) = 0.0010,
  TLMINB(3) = 365.0,
  TGINB       = 365.00,
  PSFINB      = 1.0D+5,
  ARCWIB      = 97.00,
  ASMINB(7) = 0.05,
  ASMINB(8) = 0.45,
  TSINB(7) = 365.00,
  TSINB(8) = 365.00,
  RLM0IB(1) =6*0.001, RGB0IB=0.001, XENRIB(1)=6*1.0,
  RLM0IB(4) =0.0021, RLMINB(4)=0.0021,
RLMAXB(4)=0.0021,
  RLM0IB(3) =0.0001, RLMINB(3)=0.000001,
RLMAXB(3)=0.0001,
 &END

######BLOCK 6 ######
 &XCWD

  VC(1,37,1) =  -5.00,
  VC(2,37,1) =  -5.00,
  VC(3,37,1) =  -5.00,
  VC(4,37,1) =  -5.00,
  VC(5,37,1) =   0.00,
  VC(6,37,1) =   0.00,

  VC(1,38,1) =  -4.90,
  VC(2,38,1) =  -4.90,
  VC(3,38,1) =  -4.90,
  VC(4,38,1) =  -4.90,
  VC(5,38,1) =   0.00,
  VC(6,38,1) =   0.00,

  VC(1,39,1) =  -4.80,
  VC(2,39,1) =  -4.80,
  VC(3,39,1) =  -4.80,
  VC(4,39,1) =  -4.80,
  VC(5,39,1) =  -4.80,
  VC(6,39,1) =   0.00,

  VC(1,40,1) =  -4.70,
  VC(2,40,1) =  -4.70,
  VC(3,40,1) =  -4.70,
  VC(4,40,1) =  -4.70,
  VC(5,40,1) =  -4.70,
  VC(6,40,1) =  -4.70,

  VC(1,41,1) =  -4.60,
  VC(2,41,1) =  -4.60,
  VC(3,41,1) =  -4.60,
  VC(4,41,1) =  -4.60,
  VC(5,41,1) =  -4.60,
  VC(6,41,1) =  -4.60,

  VC(1,42,1) =  -4.50,
  VC(2,42,1) =  -4.50,
  VC(3,42,1) =  -4.50,
  VC(4,42,1) =  -4.50,
  VC(5,42,1) =  -4.50,
  VC(6,42,1) =  -4.50,

  VC(1,43,1) =  -4.40,
  VC(2,43,1) =  -4.40,
  VC(3,43,1) =  -4.40,
  VC(4,43,1) =  -4.40,
  VC(5,43,1) =  -4.40,
  VC(6,43,1) =  -4.40,

  VC(1,44,1) =  -4.30,
  VC(2,44,1) =  -4.30,
  VC(3,44,1) =  -4.30,
  VC(4,44,1) =  -4.30,
  VC(5,44,1) =  -4.30,
  VC(6,44,1) =  -4.30,

  VC(1,45,1) =  -4.20,
  VC(2,45,1) =  -4.20,
  VC(3,45,1) =  -4.20,
  VC(4,45,1) =  -4.20,
  VC(5,45,1) =  -4.20,
  VC(6,45,1) =  -4.20,

  VC(1,46,1) =  -4.10,
  VC(2,46,1) =  -4.10,
  VC(3,46,1) =  -4.10,
  VC(4,46,1) =  -4.10,
  VC(5,46,1) =  -4.10,
  VC(6,46,1) =   0.00,


  ALC(1,37,4) =  0.170,
  ALC(2,37,4) =  0.170,
  ALC(3,37,4) =  0.170,
  ALC(4,37,4) =  0.170,
  ALC(5,37,4) =  1.0D-15,
  ALC(6,37,4) =  1.0D-15,

  ALC(1,38,4) =  0.170,
  ALC(2,38,4) =  0.170,
  ALC(3,38,4) =  0.170,
  ALC(4,38,4) =  0.170,
  ALC(5,38,4) =  1.0D-15,
  ALC(6,38,4) =  1.0D-15,

  ALC(1,39,4) =  0.170,
  ALC(2,39,4) =  0.170,
  ALC(3,39,4) =  0.170,
  ALC(4,39,4) =  0.170,
  ALC(5,39,4) =  0.170,
  ALC(6,39,4) =  1.0D-15,

  ALC(1,40,4) =  0.170,
  ALC(2,40,4) =  0.170,
  ALC(3,40,4) =  0.170,
  ALC(4,40,4) =  0.170,
  ALC(5,40,4) =  0.170,
  ALC(6,40,4) =  0.170,

  ALC(1,41,4) =  0.170,
  ALC(2,41,4) =  0.170,
  ALC(3,41,4) =  0.170,
  ALC(4,41,4) =  0.170,
  ALC(5,41,4) =  0.170,
  ALC(6,41,4) =  0.170,
```

```
  ALC(1,42,4) =  0.170,
  ALC(2,42,4) =  0.170,
  ALC(3,42,4) =  0.170,
  ALC(4,42,4) =  0.170,
  ALC(5,42,4) =  0.170,
  ALC(6,42,4) =  0.170,

  ALC(1,43,4) =  0.170,
  ALC(2,43,4) =  0.170,
  ALC(3,43,4) =  0.170,
  ALC(4,43,4) =  0.170,
  ALC(5,43,4) =  0.170,
  ALC(6,43,4) =  0.170,

  ALC(1,44,4) =  0.170,
  ALC(2,44,4) =  0.170,
  ALC(3,44,4) =  0.170,
  ALC(4,44,4) =  0.170,
  ALC(5,44,4) =  0.170,
  ALC(6,44,4) =  0.170,

  ALC(1,45,4) =  0.170,
  ALC(2,45,4) =  0.170,
  ALC(3,45,4) =  0.170,
  ALC(4,45,4) =  0.170,
  ALC(5,45,4) =  0.170,
  ALC(6,45,4) =  0.170,

  ALC(1,46,4) =  0.170,
  ALC(2,46,4) =  0.170,
  ALC(3,46,4) =  0.170,
  ALC(4,46,4) =  0.170,
  ALC(5,46,4) =  0.170,
  ALC(6,46,4) =  1.0D-15,

  TLC(1,1,4) = 1350*2300.0,

  &END

######BLOCK 7 ######
 &XEDT
  PRTC=5000,PPFC=100,DMPC=999991,BSFC=200,
  DTEOS(1,1)=300,50,3900,
  NPRINT(1)=2,
  NPAGE= 20,
  LPRGN(10) = 1,0,0,1,
  LPRGN(17) = 1,
  LPRGN(30) = 1,1,0,0,1,1,
  SN(1)='ALPLK1','ALPLK2','ALPLK3',

'ALPLK4','ALPLK5','ALPLK6','ALPGK','ALPGE','PK','IRGMK',
       'TLK1','TLK2','TLK3','TLK4','TLK5','TLK6','TGK',
       'VK1','VK2','VK3','UK1','UK2','UK3',
       'RGBK','CPK','DPK',
       'RBGK1','RBGK2','RBGK3','RBGK4','RBGK5',

'RBLK1','RBLK2','RBLK3','RBLK4','RBLK5','RBLK6','RBLK7','
RBLK8',
       'RBLK9','RBLK10',
       'ALPGEK',
       'TSAT1','TSAT2','TSAT3',
       'PGMK1','PGMK2','PGMK3','PGMK4',

 &END

###### BLOCK 8 ######
 &XEOS
   ISAE(2,1)     =    1,
   IMRK(2,1)     =    0,
   ISPN(2,1)     =    0,
  BETA(2,1)      =-1.00000D+00,
  ESOLUS(2,1)    = 1.56000D+06,
  ELIQUS(2,1)    = 1.56520D+06,
  CVG(2,1)       = 5.20000D+02,
  TCRT(2,1)      = 8.50000D+03,
  RUGM(2,1)      = 8.66636D+01,
  WM(2,1)        = 9.59400D+01,
  TSOLUS(2,1)    = 3.00000D+03,
  TLIQUS(2,1)    = 3.01000D+03,
  ELIQG(2,1)     = 6.75606D+06,
  PCRT(2,1)      = 1.60651D+10,
  ELIQGD(2,1)    = 6.75606D+06,
  VSOLUS(2,1)    = 9.80392D-05,
  VLIQUS(2,1)    = 9.80392D-05,
  ECRT(2,1)      = 4.42000D+06,
  ROCRT(2,1)     = 1.02000D+04,
  PSMIN(2,1)     = 1.85005D-05,
  DTDPS(2,1)     = 0.00000D+00,
  DVDPS(2,1)     =-1.53787D-15,
  DTDPC(2,1)     = 0.00000D+00,
  AS(1,2,1)      = 1.00000D+00, 0.00000D+00, 0.00000D+00,
  BS(1,2,1)      = 0.00000D+00, 0.00000D+00, 0.00000D+00,
  AL(1,2,1)      = 1.00000D+00, 0.00000D+00, 0.00000D+00,
                   2.82392D+00, 0.00000D+00, 0.00000D+00,
  BL(1,2,1)      = 3.09007D+01, 0.00000D+00,-6.29066D+04,
                   0.00000D+00,
  CL(1,2,1)      = 0.00000D+00, 0.00000D+00, 0.00000D+00,
                   0.00000D+00,
  DL(1,2,1)      = 0.00000D+00, 0.00000D+00, 0.00000D+00,
                   2.82392D+00, 0.00000D+00, 0.00000D+00,
  FL(1,2,1)      = 0.00000D+00, 0.00000D+00, 0.00000D+00,
                   0.00000D+00, 0.00000D+00, 0.00000D+00,
  DG(1,2,1)      = 0.00000D+00, 0.00000D+00,
  FG(1,2,1)      = 0.00000D+00, 0.00000D+00, 0.00000D+00,
                   0.00000D+00,
  AG(1,2,1)      = 0.00000D+00, 0.00000D+00, 1.00000D+00,
                   0.00000D+00,
  BG(1,2,1)      = 3.29486D-12, 6.29066D+04, 0.00000D+00,
                   0.00000D+00, 0.00000D+00, 0.00000D+00,
  CG(1,2,1)      = 5.20000D+02, 0.00000D+00, 0.00000D+00,
                   1.00000D+00, 0.00000D+00, 0.00000D+00,
  ASAT(1,2,1)    = 4.91215D-04,-1.58966D-05, 0.00000D+00,
                   0.00000D+00,
  BSAT(1,2,1)    = 0.00000D+00, 0.00000D+00, 0.00000D+00,
                   1.00000D+00, 0.00000D+00, 0.00000D+00,
  CSAT(1,2,1)    = 5.20000D+02, 0.00000D+00, 0.00000D+00,
                   1.00000D+00, 0.00000D+00, 0.00000D+00,
 &END

###### BLOCK 9 ###### ---- ORIFICE
 &XMXF

  CDD = 1.0,
  CCD = 1.0,
  CORFZN(1,54) =     2.27,
  CORFZN(2,54) =     2.27,
  CORFZN(3,54) =     2.27,
  CORFZN(4,54) =     2.27,

 &END

###### BLOCK 10 ######
 &XIFA
  DHPOOL   =   1.00,
  RLMIN(1)=0.0021, RLMAX(1)=0.0021,
  RLMIN(4)=0.0021, RLMAX(4)=0.0021,
  CLL(1,3)=1.00,
  CLL(4,3)=1.00,
 &END

###### BLOCK 11 ######
 &XHTC
  HFCLP(1,3) =  5.10000D-01,
  HFCLP(2,3) =  5.00000D-01,
  HFCLP(3,3) =  4.00000D-01,
  HFCLP(4,3) =  1.50000D-02,
  HFCLP(5,3) =  3.33333D-01,

  HNCLP(1,3) =  5.00000D-01,
  HNCLP(2,3) =  2.50000D-01,
```

```
  HNCLP(3,3) =   1.18000D-00,

  HFCLS(1,3) =  2.30000D-02,
  HFCLS(2,3) =  8.00000D-01,
  HFCLS(3,3) =  3.00000D-01,

  FILMIN      =  1.00000D-04,
  CMFB        =  0.64,

  HCDGS       =  5.0,
  HCDLAS(1)   =  3*2.0,

 &END

###### BLOCK 12 ######
 &XBND
  NBC          =     0,
  LBCSET       =     29*0,1450*0,0,4*1,24*0,
 &END

 &XBND
  NBC          =     1,
  LBCS         =     2,
  LBCP         =     4,
  PTAB(1)      =     1.00D5, 1.00D5, 1.00D5, 1.00D5,
  PTME(1)      =    -0.500,  0.000,  0.5000, 2.0000,
 &END

###### BLOCK 13 ###### AKPS = 88-142 W/MK

 &XTPP
  AKPL(1,2,1)  = 6.60000D+01, 0.00000D+00, 0.00000D+00,
  AKPS(1,2,1)  = 6.60000D+01, 0.00000D+00, 0.00000D+00,
                 0.00000D+00, 0.00000D+00,

  EMSVS(2,1)   =     0.3,
  EMSVL(2,1)   =     0.3,
  EMSVL(2,3)   =     0.95,
 &END

###### BLOCK 15 ######
 &XHMT
  FMTLG = 1.0D-4,
  PHI   = 0.01,
  MIVC  =290,
  IVCHLG=250,
  FTSTL = 0.6,
  FTSTH = 0.95,
 &END
###### BLOCK 17 ######
 &XMSC
  COURTN       =  0.3,
  OPTPIT       =  9,
  MPIT         =  900,
  MAXITC       =  300,
  EPSVEL       =  1.0D-04,
  EPSP         =  1.0D-01,
  EPSRO        =  1.0D-04,
  EPST         =  1.0,
  EPSPCV       =  1.0D-04,
 &END
###### BLOCK 18 ######
 &XERG
  REGN         =     1,
  REGC(1,1)    =     1,
  REGC(2,1)    =     1,
  REGC(3,1)    =    27,
  REGC(4,1)    =    50,
  MATEOS(1,1) =     2,
  MATEOS(2,1) =     2,
  MATEOS(3,1) =     2,
  MATEOS(4,1) =     2,
  MATEOS(5,1) =     2,
 &END
```